Università del Piemonte Orientale "Amedeo Avogadro"

Scuola di Dottorato XXX Ciclo Chemistry and Biology
Coordinatore Prof. Luigi Panza

Increasing Eukaryotic Initiation Factor (eIF6) gene dosage stimulates global translation and induces a transcriptional and metabolic rewiring that blocks Programmed Cell Death

Supervisor: Prof. Mauro Patrone

Co-Supervisor: Prof. Stefano Biffo

Co-Supervisor: Dr. Piera Calamita

Candidata

Arianna Russo

Anno Accademico 2016-2017

Arianna Russo: *Increasing Eukaryotic Initiation Factor (eIF6) gene dosage stimulates global translation and induces a transcriptional and metabolic rewiring that blocks Programmed Cell Death,* Tesi di Dottorato, Marzo 2018.

La scienza ha una grande bellezza. Uno studioso nel suo laboratorio non è solo un tecnico, è anche un bambino messo di fronte a fenomeni naturali che lo impressionano come una fiaba. (Marie Curie, 1934)

Contents

Introduction

Ribosome Biogenesis and Protein Synthesis

Translation, or protein synthesis, is defined as the process in which mRNAs, previously transcribed from DNA and processed, are decoded by ribosomes to make proteins. Ribosomes are essential macromolecular machines necessary to synthetize proteins from information encoded by mRNAs. The active ribosome is called 80S, from its apparent sedimentation velocity, and is composed of two subunits, namely the 60S (large) and 40S (small). These two subunits are made of ribosomal RNA (rRNA) and Ribosomal Proteins (RPs), in particular the 60S contains three rRNAs (28S, 5S and 5.8S) and 46 RPs, while the 40S is formed by only a single rRNA (18S) and 33 RPs [1, 2].

Ribosome biogenesis, one of the most energy-demanding process in cell [3], begins in the nucleolus with the transcription by RNAPolI of a polycystronic gene encoding 28S, 18S and 5.8S rRNA molecules, producing the 47S precursor. For the transcription of this precursor in mammals, at least three basal factors are necessary: the Transcription Initiation Factor I (TIF-I), the Selectivity factor 1 (SL1), and the Upstream Binding Factor (UBF) [4, 5]. The RPs' mRNAs are transcribed by RNAPolII, then they are translated in the cytoplasm. RPs then are imported in the nucleolus where they assemble with the rRNAs [6] and with the 5S rRNA, transcribed separately (by RNAPolIII). All together they form the 90S precursor, that is subsequentely cleaved in 66S and 43S pre-ribosomes. These pre-ribosomes are then transported into the cytoplasm to complete their maturation. Ribosome biogenesis is

a process strictly regulated and its rate is controlled by cell proliferation-controlling processes [7].

Translation can be divided in four major steps: initiation, elongation, termination and ribosomal recycling. Each of these steps is assisted by protein factors, called eukaryotic initiation factors (eIFs), eukaryotic elongation factors (eEFs) and eukaryotic termination factors (eRFs), which transiently associate with the ribosome and/or the mRNA. Translation initiation consists in a series of events that leads up to the recruitment of an elongation-competent 80S ribosome at the start codon of an mRNA. The elongation phase consists in the polypeptide synthesis. Lastly, the completed polypeptide is released after the ribosome encounters a stop codon during translation termination [8]. Translation is the most energy consuming process in cells [9] and thus need to be tightly regulated. The most regulated step of translation is the initiation. Indeed, while only a few factors are dedicated to elongation and termination, more than 25 proteins are needed to guarantee a proper translation initiation [10]. Translational regulation can be divided into global regulation of translation and mRNA specific regulation [11]: global regulation affects the translation efficiency of most mRNAs through a general tuning of translation, while mRNA specific regulation affects the translation of specific mRNAs. Global regulation of translation is generally mediated through modifications of translation initiation factors that transform the information from external compartments to the cell.

Notably, translation has been found altered in cancer cells [12, 13]. Indeed, recent works have shown that the translational machinery plays an active role in transformation and tumor malignancy, suggesting that it can be a therapeutic target [14, 15].

Eukaryotic Initiation Factor 6 (eIF6)

Eukaryotic Initiation Factor 6 (eIF6), also known as integrin β4 binding protein or p27BBP, is a unique conserved protein, with no motifs shared with other proteins. The protein is 245 aminoacids long and displays a striking 95% identity between its

human and *Drosophila* homologs [16]. The structure of eIF6 was resolved by X-ray cristallography [17]: eIF6 is a higly rigid protein, organized with a cyclic fold known as pentein or star-like structure (Figure 1). This cyclic structure is made by five stretches of α/β subdomains arranged to form a five-axis pseudosymmetry. Inside this structure, sixteen well ordered water molecules are hosted, with limited motility.

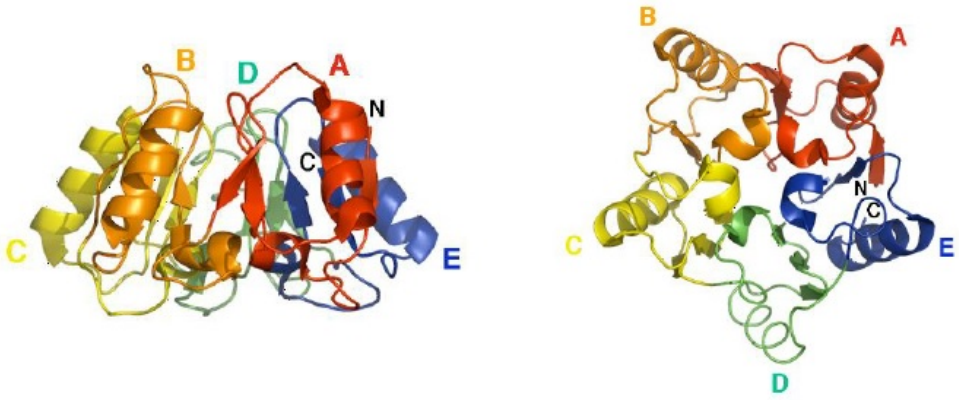

Figure 1: Structure of eIF6. The protein has a unique star-like structure known as pentein, formed by five quasi-indentical subdomains (from A to E) arranged in a pseudosymmetry

It has been demonstrated that eIF6 binds the large subunit of the ribosome, 60S, in the intersubunit space, and it is also able to interact with the C-terminal chain of the ribosomal protein L23 (rpL23) [18]. In addition to rpL23, to help the binding between eIF6 and the 60S, eIF6 also interacts with the sarcin loop of rpL24. Due to its position in the intersubunit space, that causes a steric hindrance, the binding of eIF6 to the 60S prevents its joining with the small ribosomal subunit, the 40S. Actually, eIF6 was first identified for its anti-association activity in calf liver [19] and in wheat germ [20]. It is therefore reasonable hypothesize that eIF6 activity is relevant for translational control. Then, if eIF6 prevents the joining of the two ribosomal subunits, to starts translation eIF6 needs to be released from the 60S. For this event, two models have been proposed (Figure 2):

- After the traslocation from the nucleus to the cytoplasm of the complex eIF6-60S, the interaction with the Shwachman-Bodian-Diamond Syndrome protein

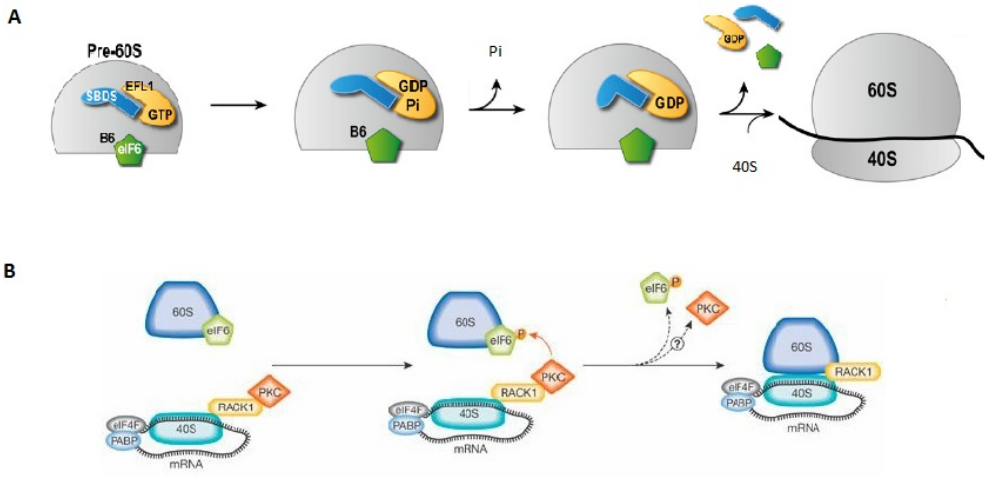

Figure 2: Models of eIF6 release from the 60S and subsequent initiation of translation. A) Interaction of the complex eIF6-60S with SBDS and Efl1p leads to a conformational change that causes the release of eIF6 from the 60S. B) Activated PKC interacts with RACK1, on the 40S. PKC phosphorylates eIF6 on its C-terminus, determining a conformational change and the consequent release. Adapted from [26] (A) and from [27] (B).

(SBDS) and the GTPase Efl1p leads to the allosteric change of the 60S itself and causes the displacement of eIF6 [21]. This mechanism is relevant to the maturation of the 60S [22], but it is still unclear if it is also involved in the translational control.

- Phosphorylation of eIF6 by the PKCβII causes a conformational change in eIF6 itself that leads to its release from the 60S [23, 24]. In this model, activated PKC translocates from endomembranes and interacts with RACK1, a scaffold protein docked on the 40S. This complex comes in the vicinity of 60S bound to eIF6, and PKC phosphorylates eIF6 on its C-terminus, determining the release [25]. Intriguingly, the C-terminus of eIF6 contains several phosphorylation sites.

Moreover, besides this anti-association activity, several studies have demonstrated that, unlike other translation initiation factors, eIF6 has other functions: indeed it is also necessary for biogenesis of the 60S [27], and therefore is localized both in the cytoplasm and in the nucleolus. Intriguingly, during evolution *eif6* gene has never been subjected to genetic duplication, strongly suggesting the need of a tight

regulation of eIF6 protein levels. Indeed, human eIF6 is costitutively expressed *in vitro*, but highly modulated *in vivo*: levels of eIF6 varies among different organs. Studies on many metazoan tissues demonstrated that the protein is higly expressed in brain but has low levels in muscles. Furthermore, eIF6 shows high levels in stem or cycling cells, but is almost undetectable in several post-mitotic cells [28]. These observations also suggest that it might be difficult to generate *in vivo* models with altered levels of eIF6 [29].

eIF6 is upregulated in cancer

Protein synthesis is the most energy consuming process in cell [9] and has been demonstrated that it largely contributes to gene expression variations [30]. It is reasonable then that it needs to be tightly regulated and that alterations in translational control could be causative of many pathologies. In particular, it has been recently uncovered how alterations of gene dosage in both Ribosomal Proteins (RPs) and translation eukaryotic Initiation Factors (eIFs) are involved in cancer [31], even if, until a few years ago, alterations to the ribosomal machinery have been considered only a by-product of transformation and tumor growth rather than causative of cancer. However, the oncogenic role of an initiation translation factor, eIF4E, has been known since 1990 [32]. Interestingly, while overexpression of eIF4E leads to only a mild increase in global translational rate, a specific subset of mRNAs are more translated in condition of eIF4E increased levels, and these include oncogenes as c-MYC, anti-apoptotic factors as BCL-xL and proangiogenic factors like VEGFA [33]. It is no surprise then to find eIF4E levels increased in many cancer types, such as head and neck, breast, prostate, leukemias and colon [15]. The list of eIF4E overexpressing cancer is growing continually [34–36]. eIF4E overexpression is only an example of how cancer cells can benefit from deregulation of gene dosage of factors involved in translational control, and many other examples could be made. The role of eIF6 in cancer is less well established. It has been demonstrated that eIF6 is upregulated or hyperphosphorylated in several cancer types (Figure 3),

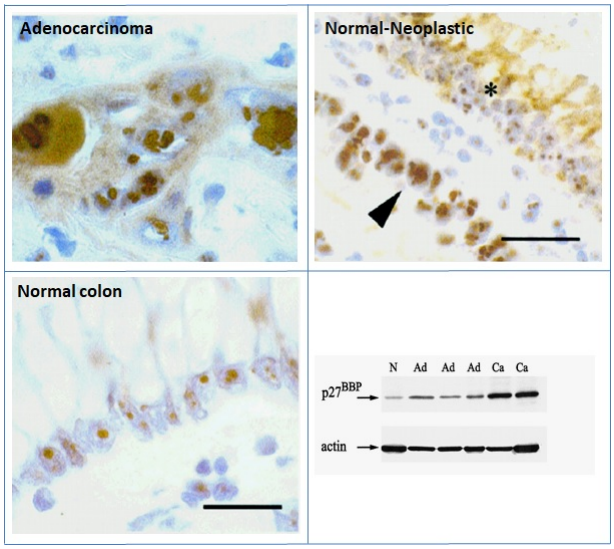

Figure 3: eIF6 is upregulated in colon adenocarcinoma. Adapted from [45]

such as head and neck [37], lung metastasis [38], acute promyelocitic leukemia [39] and malignant mesothelioma [16, 40]. Moreover, amplification of *eif6* gene has been found in luminal breast cancer [41]. Conversely, it has been observed that haploinsufficiency of eIF6 results in reduced MYC or HRAS-mediated oncogenic transformation [42]. Interestingly, MYC-induced lymphomagenesis is strikingly reduced in murine lymphoma with halved eIF6 levels, resulting in an astonishing prolonged tumor free survival in the absence of negative side effects [43]. Indeed, mice haploinsufficient for eIF6 are viable and fertile, even if leaner respect to their littermates [44]. Still, the mechanism(s) that explain eIF6 overexpression in cancer remains to be pinpointed, and also the early effects of *eif6* increased gene dosage are still unclear.

Drosophila melanogaster is an outstanding model organism

Drosophila melanogaster (Figure 4) has been used as a model organism for more than a century. The first documented use of this organism in a lab dates back to no less than 1901, in the lab of William Castle, but the undisputed champion of

Figure 4: *Drosophila* male and female. It is really easy to distinguish males and females in *Drosophila*. Females are slightly bigger, and have a lighter pigmentation. Genitalia are of course a way to distinguish sexes: *Drosophila* genitalia are at the end of the abdomen. Moreover, only males possess a structure known as sex combs, tiny hair on the legs.

Drosophila research is Thomas Hunt Morgan, who started its pioneering work in 1910 [46]. His studies granted him the Nobel Prize in Physiology or Medicine in 1933, for his discoveries about the role of chromosomes in heredity [47]. *Drosophila* was then used to undercover mechanisms of pattern formation [48], development of the nervous system and even to model human diseases [49]. *Drosophila* possesses the main characteristics of all model organisms: a short life-cycle, a simple anatomy, the ability to produce copious progeny in just few days and it is easy and cheap to nurture. It is not to understimate that ethical and safety issues are minimal when using *Drosophila*.

Like all holometabolous insects, *Drosophila* undergoes a life cycle made up of four stages: embryo, larva, pupa and adult (Figure 5). The duration of this life cycle is strictly dependent on the temperature: development lasts 9 days at 25°C, while at 18°C it proceeds slower. At 25°C, embryos take up rougly a day before hatching in a larva that eats and grows for over five days, undergoing three moltings. After that, the larva stops moving and becomes a pupa, that gives rise to an adult through metamorphosis after four days. This relative short life cycle allows to perform in just a few weeks genetic experiments that would takes months or even years in zebrafish

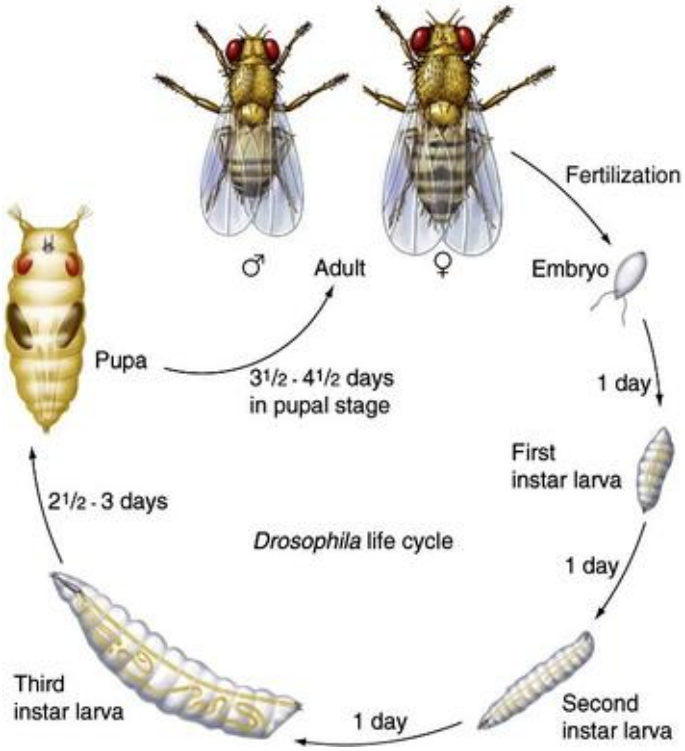

Figure 5: *Drosophila* life cycle. As every holometabolous insect, *Drosophila* undergoes four stages during its life cycle: embryo, larva (with three moltings), pupa and adult. From the fertilization of the embryo to the adult stage, development lasts nine days at 25°C.

or mouse. Moreover, each female lay hundreds of eggs during its life, allowing the generation of a large number of offspring.

Another edge of *Drosophila* as a model organism is its powerful genetics. *Drosophila* possesses only four pairs of chromosomes and its genome sequence has been released in March 2000 [50], and it is accessible, together with annotations, via "Flybase" [51]. Among the 14000 estimated *Drosophila* genes, 75% of disease human genes have been found [52], legitimating *Drosophila* also for medical research. In addition to this bulk of information, there are many genetics tools that can be used in *Drosophila*. Maybe one of the most elegant genetic tool used in *Drosophila* is the GAL4/UAS system [53] (Figure 6). GAL4 encodes a protein of 881 aminoacids, firstly found in yeast, that acts as a transcriptional activator upon a genomic sequence, the Upstream Activating Sequence (UAS), which acts as an enhancer element. In this system, the GAL4 gene is inserted nearby a promoter, providing a temporal and spatial

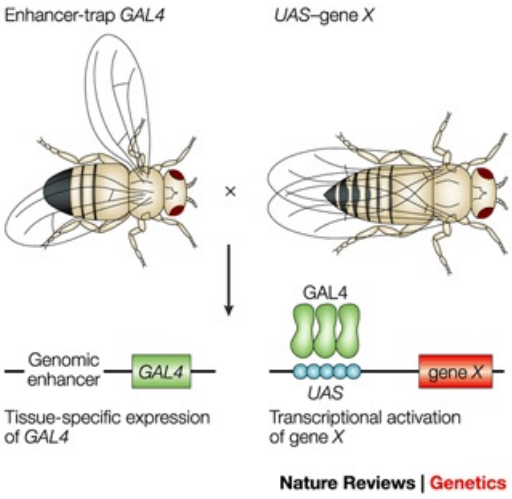

Figure 6: GAL4/UAS system. The yeast transcriptional activator Gal4 can be used to regulate gene expression in *Drosophila* by inserting the Upstream Activating Sequence (UAS) to which it binds next to a gene of interest (gene X). The GAL4 gene has been inserted at random positions in the *Drosophila* genome to generate 'enhancer-trap' lines that express GAL4 under the control of nearby genomic enhancers. Therefore, the expression of gene X can be driven in any of these patterns by crossing the appropriate GAL4 enhancer-trap line to flies that carry the UAS–gene X transgene. Adapted from [54].

expression of the protein GAL4. When expressed, GAL4 induces the expression of a gene that is under the UAS control. This method represents an important tool for controlled protein expression, both in temporal and spatial manner.

The *Drosophila melanogaster* eye and its adult structure

Drosophila melanogaster eye, a stunningly beautiful structure, has been studied for more than a century, and has been used as a model system to understand several physiological processes, for example tissue specification, organogenesis, cell proliferation, specification and differentiation, planar cell polarity and programmed cell death. From the identification of the first white eyed fly in a sea of wild type red-eyed flies (Figure 7), this organ has been a favourite model for geneticists, cell and developmental biologists. In this choice, great importance had the knowledge that flies can live without eyes. During evolution, two different types of retina have emerged. Larger animals, including most vertebrates, possess a single camera

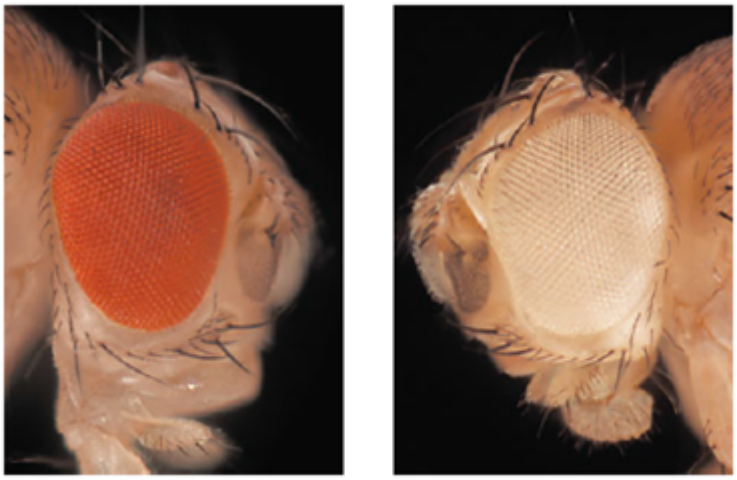

Figure 7: *Drosophila* adult compound eye. Stereomicroscope images of a wild type (red) eye and a mutant (white) one. The isolation of a mutant white eye by T. H. Morgan was groundbreaking in *Drosophila* research and more generally in the understanding of hereditariness.

eye, made of three components: a lens, a retina and a pigment layer. This kind of eye is sensitive and with a high resolving power, but has a major downside: lens and retina need to have a minimum distance between each other, and this is why simple camera eyes are presented only by larger animals. Insects and other smaller animals, instead, present compound eyes, made up of a cluster of identical units, called ommatidia, each one made of the same components of simple camera eyes, but compressed and compartimentalized to fit into tiny heads. In spite of the great difference in appereance between simple and compound eyes, they share many molecular factors required for their development and their function, so the initial polyphyletic hypothesis (indipendent appeareance of a structure multiple time during evolution) was recently excluded.

Drosophila compound eye contains ~800 ommatidia, each one composed of eight neuronal cells, the photoreceptors (PRCs), named from R1 to R8, photosensitive cells that transmit visual stimuli projecting directly to the brain. PRCs are capped by four glial-like, lens secreting cells, the cone cells, and two primary pigment cells. A hexagonal lattice of secondary and tertiary pigment cells, also known as InterOmmatidial Cells (IOCs) surround each ommatidium, preventing the passage

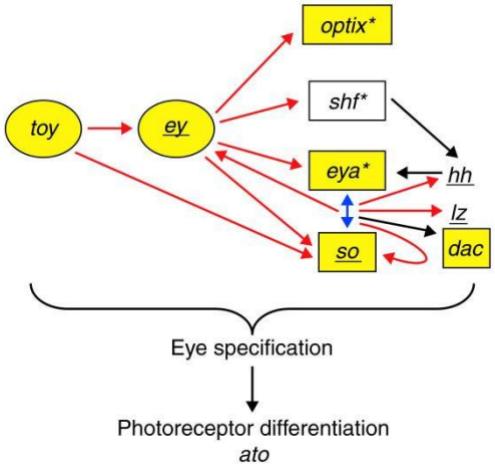

Figure 8: The retinal determination network (RDN). Members of the RDN are indicated on a yellow background. Toy activates expression of ey as well as so. Ey activates expression of so, eya*, optix* and shf*. Eya and So interact to directly activate expression of their targets: lz, hh, ey and so, as well as indirectly activating expression of the downstream gene dac. Members of the RDN are required for eye specification, upstream of photoreceptors specification and differentiation, with ato functioning to regulate specification of the first photoreceptor cell, R8. Adapted from [56].

of light between ommatidia. Finally, at every other apex of each ommatidium, there is another structure, the bristle, a mechanosensory organ [55]. The arrangment of cells into each ommatidium, and the overall arrangment of ommatidia on the plane is astonishingly precise, forming a cristalline-like structure. Any perturbation during development results in the disruption of the structure. This peculiarity, coupled with the dispensability of the eyes for the flies viability, allowed for the discovery of a plethora of mutations in genes involved in different aspects of this organization, such as the number of PRCs, their morphology and function. Indeed, mutations even only in one gene involved in the development of this structure can cause the appereance of a easily identified phenotype, known as rough, or also in the complete absence of the eye.

Overall, the entire ommatidial structure is about 100 µm long. PRCs are functionally divided in two classes: outer PRCs (from R1 to R6) are important for motion detection and vision under dim light condition [57]. Inner PRCs instead, namely R7 and R8, function under bright light condition and are responsible for

color discrimination. Another major difference between outer and inner PRCs is the lenght of their projecting axons: outer PRCs have slightly longer axons that span the entire lenght of the ommatidial structure and project their axons to the lamina, while inner PRCs are shorter and synapse in the medulla [58]. The light sensitive organelle is called rhabdomere, and is an elongated apical structure of tightly packed microvilli [59]. These microvilli harbor the rhodopsins, which are the visual pigments and that are also required for the building and maintainance of the rhabdomere structure itself [60]. There are different isoforms of rhodopsin, each one expressed in different PRCs: all outer PRCs express rhodopsin 1 (Rh1), which detects a broad wavelenght [61]. In contrast, inner PRCs express a complex pattern of rhodopsins to maximize the range of wavelenght they can detect. R7 cells express Rh 3 and/or Rh4, UV-sensitive opsins, while R8 cells can express Rh3 or Rh6, which are instead green sensitive [62].

Drosophila eye development

Many adult *Drosophila* organs emerge from larval structures known as imaginal discs (from the latin word *imago*, adult insect). The eye is no exception, deriving from an epithilial monolayer known as the eye-antennal imaginal disc, that gives rise to most of the *Drosophila* head structures, from eyes and ocelli of the visual system, to head epidermis and olfactory organs [63]. The eye imaginal disc derives from a small subset of cells set aside during embryogenesis, that continue to proliferate during the three larval stages, while the organism feeds and grows. This proliferation depends on the action of a network of six transcription factors (*ey, toy, optix so, eya, dac*), known as retinal determination factors [64], also active during mammalian eye establishment (Figure 8). These factors are necessary for both proliferation and cell fate specification through interaction with many other genes [65]. The knowledge that the same factors are necessary for the specification of both simple camera and compound eyes strenghtens the monophyletyc hypothesis for the emergence of eyes during evolution. Interestingly, the expression of these genes in other imaginal discs

can drive the development of ectopic eyes.

As said, the eye-antennal imaginal disc gives rise to both eye and antenna. The factor responsible for the definition of the eye field is *eyeless* (*ey*), which expression is lost during second larval instar from the antennal section of the disc, that is instead specified by the expression of Cut. *ey* acts in coordination with other factors to promote both proliferation and specification of eye fate. During the first two larval stages cells divide homogeneously. The first sign of differentiation appears during third larval instar: a physical indentation called Morphogenetic Furrow (MF) appears at the posterior edge of the eye disc and moves from posterior to anterior (Figure 9), due to the expression of two morphogenes, *Decapentapegic* (Dpp), which is expressed anteriorly of the MF, and *Hedgehog* (Hh), posteriorly [66]. This physical indentation is caused by a costriction of the apycal part of the cell and a contration of the apicobasal axis [67]. Many factors partecipate to this dramatic change in cellular shape: microtubles, filamentous actin and non-muscle myosin cause the cells to first enter and then be realesed from this furrow-like state, causing the posterior-to-anterior sweep of this structure [68]. The MF divides the eye disc in two disctint regions: anteriorly cells continue to proliferate, while cells in the MF itself arrest their cell cycle in G1 phase and start their differentiation posteriorly of the MF. In this wave of differentiation ommatidia are built in a fascinating manner, one cell at a time, through a network of local signal. The first cell to be specified is a photoreceptor, R8, through the expression of a basic helix-loop-helix (HLH) transcription factor, *atonal* (*ato*), induced by Hh and Dpp. Loss of *ato* causes the complete elimination of PRCs development [69], even if th MF is present and sweeps the disc [70]. From surrounding undifferentiated cells, specified R8 recreuits stepwise and pairwise other four PRCs: first R2 and R5, then R3 and R4. At this point, the five-cell precluster is complete; cells still uncommitted undergo a last mitosis, known as the second mitotic wave, from which originate all the other cells that put together an ommatidium. Without the second mitotic wave, differentiation continues normally, but ommatidia will lack of some cells, hinting that this last round of

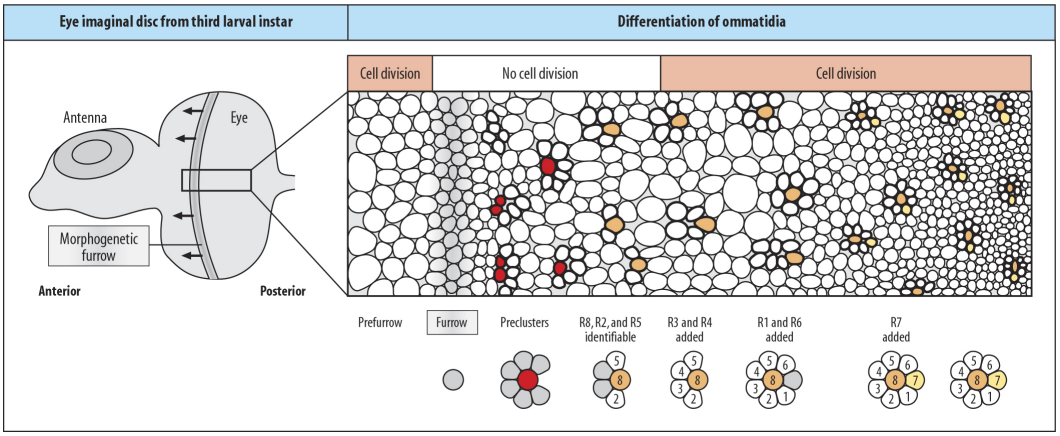

Figure 9: Differentiation starts after the Morphogenetic Furrow. The MF divides the eye disc in two disctint regions: anteriorly cells continue to proliferate, while cells in the MF itself arrest their cell cycle in G1 phase and start their differentiation posteriorly of the MF. In this wave of differentiation ommatidia are built in one cell at a time, through a network of local signal, starting from the founder photoreceptor, R8. During the larva stage, all photoreceptors are specifid, together with cone cells.

division is necessary only to generate a great quantity of cells [71]. From this point of view, then it can be said that the first mitotic wave (before the emergence of the MF) sets the limit of how many ommatidia can be generated, while the second mitotic wave is responsible of the number of cells that each ommatidium possesses [72]. Then, from the pool of cells derived from the second mitotic wave, the last three PRCs are recruited, first R1 and R6, and lastly R7 [73]. The last group of cells that are committed during the third larval instar is the group of the four non-neuronal, glial-like cone cells, also known as Semper cells. The main regulator of cone cells differentiation is *DPax2*, also known as *sparkling*, as its mutation causes a glossy eye, or *shaven*, for the absence of bristles [74–76]. Although many progresses have been made in the understanding of how cone cells are recruited and specified, the exact mechanism(s) is still elusive.

Cone cells are the last cells to be specified during larval stages. The last part of eye development takes place during pupal stages. The last cells that will be specified during *Drosophila* eye development are pigment cells. Although these cells derive from the second mitotic wave, they are differentiated only during the first half of the pupal development [77]. As for cone cells, it is still unclear how pigment

cells are committed, even though it is now clear that primary pigment cells are recruited directly by cone cells, though a local signal pathway, dependent on the secretion of *Delta* (Dl). Dl is produced in cone cells under the control of the EGF receptor pathway, then secreted to activate non-autonomously the Notch pathway in neighbouring cells, that under this signal will differentiate in primary pigment cells [78]. Still, the transcriptional targets downstream of Notch signal that confer the primary pigment cell fate remain to be identified. However, this pathway is not sufficient to trigger primary pigment cells specification *per se*. Cells that will become primary pigment cells must also express a trascription factor belonging to the RUNX family, Lozenge, in order to be correctly committed [78]. In addition, other factors have a role in this determination: trascription of many genes necessary in this event is controlled by the retinal determination factors Eyes absent (Eya) and Sine Oculis (So) [79]. The last cells that will be specified are secondary and tertiary pigment cells. The factors necessary for this last cell fate commitment are still more evasive than the ones necessary for primary pigment cells, even if now the role of Notch and EGF Receptor pathways have been demonstrated [80–82]. During this last event of cell fate commitment, a wave of spatially restricted programmed cell death is of great importance to determine the right cristal-like structure of the fly retina.

The apoptotic wave during pupal stages determines the cristalline structure of *Drosophila* eye

Apoptosis has many roles during development of all metazoan. These include the elimination of cells and tissue that are obsolete, the removal of aberrant cells that could potentially be harmful to the organism and the generation of complex tissue architecture [83]. During *Drosophila* eye development, the precise adult structure is obtained also through a wave of Programmed Cell Death (PCD) that during pupal stages sweeps the developing retina to eliminate cells in excess produced by the second mitotic wave [82]. Whethever the signals that lead to the recognition

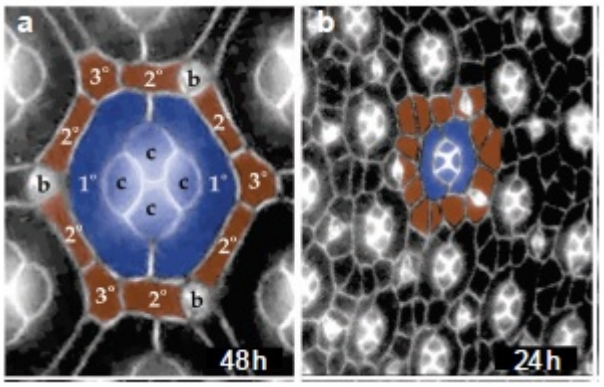

Figure 10: Apoptosis shapes the pupal retina. During pupal stages, apoptosis of IOCs determines the right number of cells for each ommatidium. In A), wild type retina at 48 hours APF, in B) at 24 hours APF. Adapted from [98].

of which cells need to be removed is, once the apoptosis is triggered it inevitably results in the death of the cell [84], and the key players are the same involved in mammalian apoptosis. In *Drosophila*, two initiator (or upstream) caspase have been identified, Dronc and Dredd [85–87]. It has been demonstrated that Dronc is active during pupal PCD [88] and that, similarly to its mammalian counterpart caspase 9, it forms a complex with the fly orthologue of Apaf-1 Dark [89, 90]. The activation of Dronc leads to the subsequent activation of Drice and Dcp-1, the downstream caspases active in the pupal IOCs [88]. The activity of these caspases is inhibited by the direct binding of DIAP-1 [91]. Other factors are involved in this process, such as the main proapoptotic factors in *Drosophila*, the RHG proteins consisting of Reaper (Rpr), Head involution defect (Hid) and Grim [92]. These factors' levels are regulated by several upstream signals such as stress, developmental cues or the steroid hormone ecdysone [93–95]. The main role of RHG proteins is to bind to the Drosophila inhibitor of apoptosis protein (Diap1), which is essential for keeping caspases inactivated in the absence of apoptotic stimuli [96]. When Diap1 is bound by RHG proteins, the apoptotic inhibitor itself is ubiquitinated and consequentely degradated, thus alleviating the block on caspases to allow Dronc and downstream caspase activation [97].

After specification of the primary pigment cells, the remaining Interommadial

Cells (IOCs) are arranged on the plane in two or three rows around ommatidia. Then, these cells arrange themeselves in a single row, favouring contact with the primary pigment cells [77, 99]. This arrangement is mediated by two genes: *roughest* and *hibris*, the first expressed in IOCs, the latter in primary pigment cells. The protein products of these two genes are members of the Neph/Nephrin family [100, 101], that mediates calcium-indipendent cell-cell adhesion [102, 103]. Roughest protein localizes in IOCs specifically at the interface with the primary pigment cells, while Hibris is likely localized in adherens junction of primary pigment cells [104]. These evidences suggest that Roughest and Hibris directly interact, and that this interaction is essential for the arrangement of IOCs during pupal developmental stages. After the conclusion of this sorting process, two to three cells are in excess and need to be removed. The removal of these cells is obtained through a spatially restricted wave of PCD [105] (Figure 10). The accepted model for the identification of cells in excess is that IOCs compete for a limiting survival factor. The sorting of IOCs cells is then necessary to allow this limiting survival factor to be unevenly distributed only in the right number of cells, and this is achieved through differential adhesion. Studies using direct ablation of specific cellular subtypes shed some light to what is the limiting survival factor. Indeed, direct ablation of photoreceptors had no effect on the death of IOCs, while specific removal of both cone and primary pigment cells resulted in the apoptosis of neighbouring IOCs [106]. Cone and primary pigment cells then are the cellular subtypes that send a survival signal to neighbouring IOCs. This signal was identified in Spitz, a EGF Receptor ligand. Then, IOCs express EGF Receptor, and those IOCs that are near enough to receive Spitz will survive. Notably, the activation of the EGF Receptor pathway results in the inhibition of Hid, which is, among the RGH proteins, the major inhibitor of DIAP during the pupal apoptotic wave [88]. These finding are also supported by the observation of induction of ectopic cell death upon EGF Receptor pathway inactivation [107, 108]. As in all *Drosophila* eye development, this event is not controlled by a single signal pathway, but by a network of signalling, in a fine balance of agonistic and antagonistic

signals. Indeed, cone and specified secondary and tertiary pigment cells secrete Argos, a repressor of EGF Receptor [109], and it was observed that overexpression of Argos causes increased apoptosis [108, 110]. The fact that already specified secondary and tertiary pigment cells secrete Argos is consistent with a model in which cells fated to survive ensure the destruction of their neighbouring, still uncommitted cells. There is also a second antagonistic signal, mediated by the Notch pathway. Mutations in *notch* result in less cells undergoing apoptosis [55]. Interestingly, loss of Notch causes the uniform distribution of Roughest in IOCS [111], and that results in the block of IOCs sorting.

Ecdysone is a steroid hormone essential for *Drosophila* development

Steroid hormones regulate different events in all higher eukaryotes, such as development, reproduction and metabolism [112]. The fact that regulation of many and different biological phenomena has been conserved from insects to humans suggests the importance of steroids in all metazoan. *Drosophila melanogaster* offered an outstanding model to study regulation of steroid hormones valid also for higher organisms. This is true for several reasons: as already said, *Drosophila* possesses all the useful characteristics of a model organism, such as a short life cycle, a sequenced genome and powerful genetic tools. Moreover, *Drosophila* presents giant polytene puffs in chromosomes of the salivary glands in response to ecdysone, the master regulator steroid hormone of development in *Drosophila*. Interestingly, ecdysone is homologous to mammalian steroid hormones such as estradiol (Abolaji et al. 2013).

As already said, *Drosophila* development lasts 9 days at 25°C, and, as in all holometabolous insect, consists of embryonic, three larval stages, prepupal, pupal and lastly adult (Figure 8). Each one of these stage is punctuated by a ecdysone pulse [113] (Figure 11). In the hemolymph, many forms of ecdysone can be found, but the one that is biologically active is the 20-hydroxyecdysone (20-HE) [114]. The

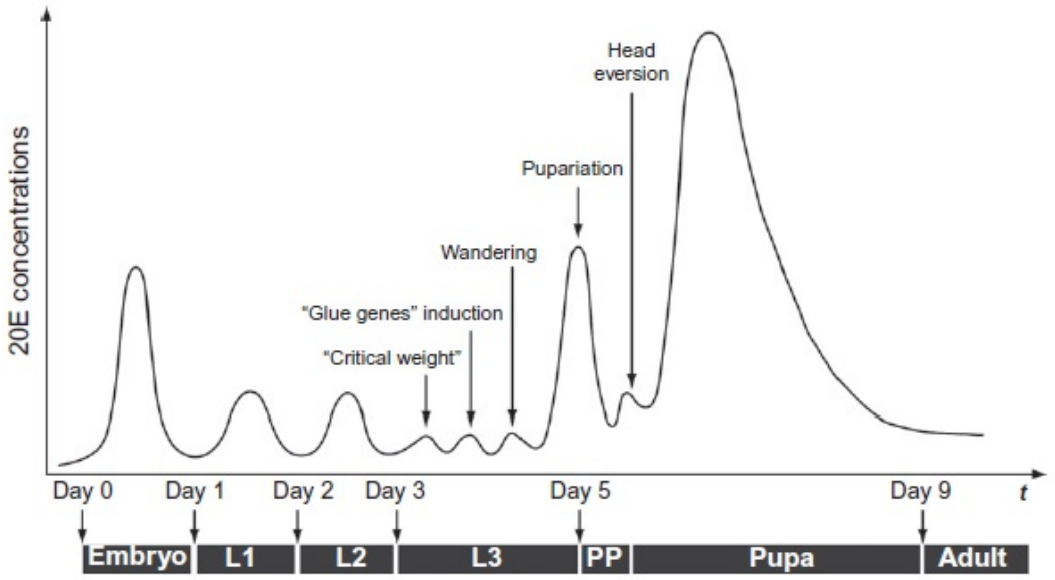

Figure 11: Ecdysone pulses during *Drosophila* development. Each developmental transition is punctuated by its own 20-HE pulse, each one with unique characteristc such as amplitude and duration, that triggers moltings and metamorphosis.

mechanism of action of 20-HE, as other lipofilic hormones, is the binding to a nuclear receptor and the consequent induction of a small subset of early genes, that are trancription factors. These early genes in turn induce the transcription of a larger subset of genes, known as late response genes, that are the ultimate responsible for the developmental changes required for metamorphosis. This paradigm is also known as the Ashburner model, from the seminal work of Michael Ashburner in 1974 [115].

As said, each developmental transition is punctuated by its own 20-HE pulse, each one with unique characteristc such as amplitude and duration. Ecdysteroids are produced in the protoracic gland, a part of a neuroendocrin organ called ring gland. The protoracic gland secretes a precursor, then every tissue takes up this precursor and converts it in the active form, the 20-HE [116]. 20-HE is produced, as many other steroid hormones, using cholesterol as a precursor [117], which is imported in the protoracic gland by Npc1a [118]. The human homologue of this genes, when mutated, causes a fatal neurodegenerative disorder, the Niemann-Pick Type C Disease, where cholesterol accumulates in lysosome [119]. The conversion

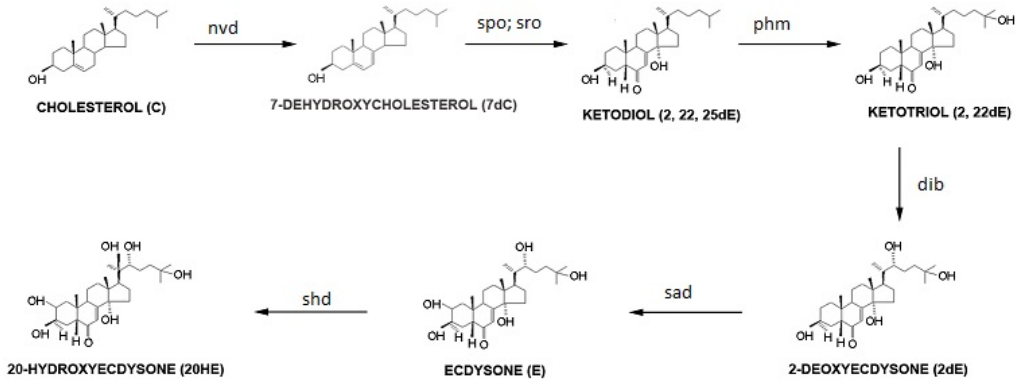

Figure 12: Ecdysone biosynthetic pathway. Biosynthesis of ecdysone takes place for the most part in the protoracic gland. The starting precursor is cholesterol, and from that a series of enzymatic reactions transforms it in ecdysone. This hormone then is secreted and every target tissue takes it and transforms it, with a final enzymatic reaction, in 20-HydroxyEcdysone.

from cholesterol to ecdysone starts with a Rieske electron oxygenase, Neverland (*nvd*), which generates 7-dehydrocholesterol [120]. After this first enzymatic reaction, 7-dehydrocholesterol is converted in 5-βketodiol, in a series of reactions of which little is known, and thus this step is called the *black box*. Enzymes believed to act in this part of the pathway are Shroud (a short-chain dehydrogenase/reductase), and two cytochrome P450 enzymes, Spookier and Cyp6t3 [121]. Other three cytochrome P450 enzymes carry out the last part of the biosynthetic pathway, namely Phantom, Disembodied and Shadow, then the ecdysone thus produced is secreted from the protoracic gland and finally transformed in its active form, 20-HE, in the target tissues, by Shade (Figure 12). These last four genes are colletively known as the Halloween genes [122].

The nuclear receptor that binds 20-HE is a heterodimer composed by Ecdysone Receptor (EcR) and Ultraspiracle (USP) [123]. The vertebrate homologue of USP is RXR [124]. Three isoforms of EcR have been identified: A, B1 and B2, with common motifs for the DNA and ligand, but with unique amino-termini [125]. Every isoform is expressed in different tissues and developmental stages, and each one is responsible for different ecdysone-induced events [125]. Three genes have been identified as early genes: BR-C, E74 and E75 [126, 127] [127], they encode for

transcription factors and, as predictable, their mutations is larval lethal, consistently with their role in metamorphosis [128]. The proteic products of these three genes are able to induce the transcription of many late genes, the actual effector of the metamorphosis. Interestingly, among events dependent on ecdysone, one of the most studied is apoptosis, necessary to destroy tissues that have become obsolete with metamorphosis. Ecdysone induces apoptosis through upregulation of the apoptosome components dark and dronc as well as drice [129]. Also other death genes are induced by high titre of ecdysone: the early response genes BR-C and E74 promote transcription of *rpr* and *hid*, two of the main proapoptotic factors in *Drosophila* [92], while downregulating the expression of the apoptosis inhibitor *diap1* (Kilpatrick et al., 2005). *rpr* and *dronc* are also direct targets of the EcR-USP complex [130].

Outline of the Thesis

Ribosomal machinery and/or translational control have been found altered in cancer cells. In particular, it has been recently uncovered how alterations of gene dosage in both Ribosomal Proteins (RPs) and translation eukaryotic Initiation Factors (eIFs) are involved in cancer, even if, until a few years ago, alterations to the ribosomal machinery have been considered only a by-product of transformation and tumor growth rather than causative of cancer. Among IFs found altered in tumours there is the Eukaryotic Initiation Factor 6 (eIF6), which regulates both ribosome biogenesis and translation initiation. It has been demonstrated that eIF6 haploinsufficiency protects mice from lymphomagenesis without adverse effects. Moreover, eIF6 has been found upregulated in many cancers types, such as colorectal, prostate, lung, leukemias and mesothelioma. In luminal breast cancer, *eif6* gene locus has been found amplified. The *eif6* gene is a single genetic locus highly conserved from yeast to humans, that has never been subjected to genetic duplication, strongly indicating the necessity of a tight regulation of its gene dosage. However, an *in vivo* study that deeply understand the early events associated with increased levels of eIF6 is still lacking. Thus, to address this issue, we applied the power of easy genetics and imaging offered by the *Drosophila melanogaster* model. Therefore, we genetically increased the levels of the *Drosophila* homologue of eIF6, DeIF6, and we deeply characterized the first *in vivo* model with high levels of DeIF6. We decided to restrict DeIF6 overexpression only in the fly eye because we found that increasing DeIF6 in the whole organism resulted in early lethalithy, a feature quite expected. We found that increasing DeIF6 levels results in a higher general translational

rate and in a rough eye phenotype dependent on an aberrant apoptosis during development. We also found that, mechanistically, eIF6 reshapes transcription and histone acetylation, disrupting a hormonal pathway, the ecdysone network. This work is the first evidence of how increased translation generates a full transcriptional and hormonal deregulation, providing new perspectives on treating cancer cells with altered *eif6* gene dosage.

Results

DeIF6 overexpression results in a rough eye phenotype

The human ($p27^{BBP}$/eIF6) and *Drosophila* (DeIF6) homologues share 95% identity [16]. We decided to take advantage of this high similarity to study the early effects of eIF6 overexpression using the *Drosophila* model. First, we overexpressed DeIF6 in *Drosophila* during early development, using the ubiquitous driver *TubGAl4*.

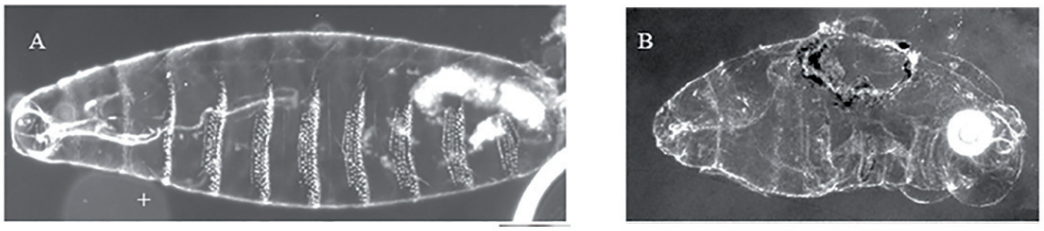

Figure 13: Overexpression of DeIF6 using the ubiquitous driver *TubGAL4* resulted in late embryonic lethality

This overexpression resulted in early embryonal lethality, thus confirming the necessity for a tight regulation of eIF6 gene dosage (Figure 13). To overcome the problem of early lethality, we then focused our studies on a dispensable organ, the eye. We overexpressed DeIF6 only in the fly eye using the *GMRGAL4* driver, and obtained an adult eye with altered morphology, also known as rough eye (Figure 14 a-b). We further characterized this phenotype, using Scansion Electron Microscopy (SEM), observing that the precise structure of the eye was completely disrupted upon DeIF6 overexpression, with flattened ommatidia and bristles arranged randomly

on the plane (Figure 14 c). Moreover, analysis of semithin tangential sections demonstrated that the roughness was not due to loss of photoreceptors, that were present and in the correct number, but to a completely aberrant arrangement of cells (Figure 14 c).

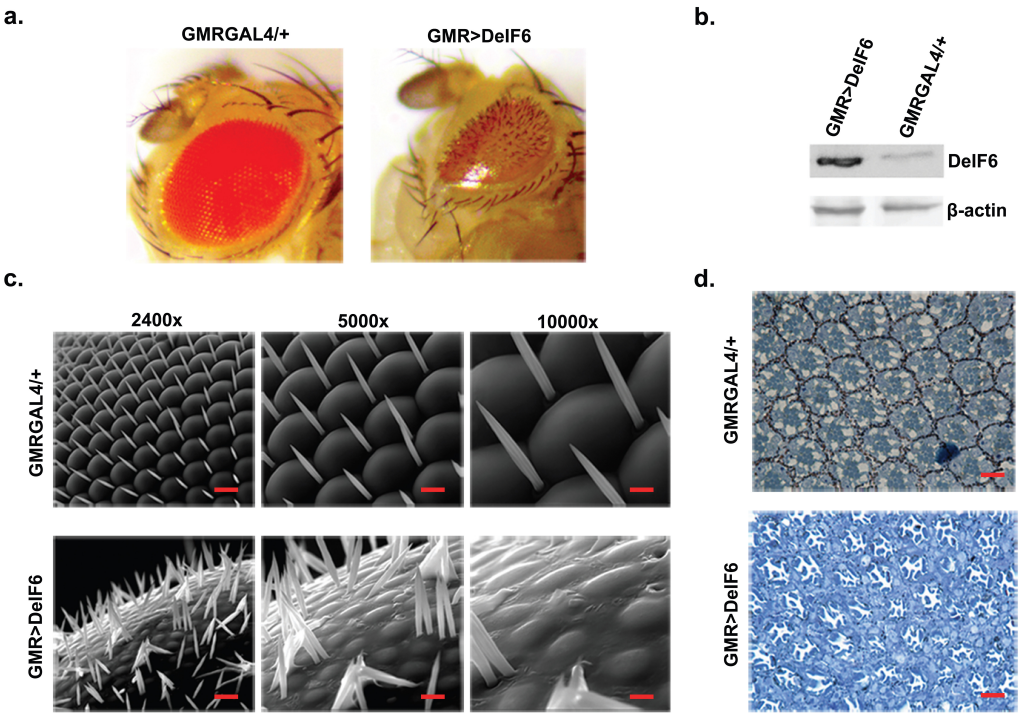

Figure 14: Overexpression of DeIF6 in the fly eye results in a rough phenotype: **a.** Stereomicroscope images of *GMRGAL4/+* and *GMR>DeIF6* showing the rough eye phenotype when DeIF6 was overexpressed. **b.** Representative western blot showing the levels of DeIF6 in *GMRGAL4/+* and *GMR>DeIF6* adult eyes. **c.** Representative SEM images of *GMRGAL4/+* and *GMR>DeIF6* adult eyes, which show the aberrant morphology exhibited by overexpressing eyes, with flattened ommatidia and randomly arranged bristles. Scale bars, in order, 10µm, 5µm and 2,5µm.**d.** Representative semithin tangential sections of *GMRGAL4/+* and *GMR>DeIF6* adult eyes. Photoreceptors are present and in the correct number, but cells' arrangment on the plane is lost. Scale bar 10µm

Increased DeIF6 gene dosage results in increased puromycin incorporation

eIF6 is a translation initiation factor involved in both biogenesis of the large subunit of the ribosome, the 60S, and in the control of initiation of translation, by

binding the 60S itself and preventing premature joining with unloaded 40S. Thus, we asked what happened to translation when eIF6 gene dosage was increased. To this end, we first evaluated the functionality of the ectopic protein, by assessing its ability to bind the 60S. Using an assay recently developed in our lab, the iRIA (Pesce et al. 2015), we observed a 25% reduction of free 60S sites when compared to control (Figure 15 a). This reduction in 60S free sites indicated that the ectopic expressed DeIF6 was able to bind the 60S, i.e. was functional. Next, we measured translational levels in eye imaginal discs using a modified SUnSET assay. In this assay, we treated eye imaginal discs *ex vivo* with puromycin, an analogue of a aminoacylated-tRNA, that is incorporated in protein nascent chains by ribosomes. Incorporated puromycin, thus, is an indicator of protein synthesis. We observed a two-fold increase in incorporated puromycin in eye imaginal discs upon DeIF6 overexpression, when compared to control (Figure 15 b-c).

To evaluate wheter this increase in puromycin incorportation was specific to *Drosophila*, or a more general effect of eIF6 increased levels, we overexpressed the human isoform of the initiation factor in HEK293 cells(Figure 16 a), and measured puromycin incorporation in condition of serum stimulation. Again, we observed a two-fold increase in puromycin incorporation, measured with a cytofluorimeter (Figure 16 b-c). Taken together, our biochemical analyses reveal that overexpressed DeIF6 is functional, and that its overexpression causes a conserved increase in general translation.

DeIF6 overexpression impairs apoptosis during pupal development

To understand how deregulation of general translation could lead to morphological defects such as the ones observed upon DeIF6 overexpression in the adult fly eye, we thoroughly analyzed eye development. The first developmental stage that we analyzed was the third larval instar, since the driver we used, the *GMRGAL4*, starts

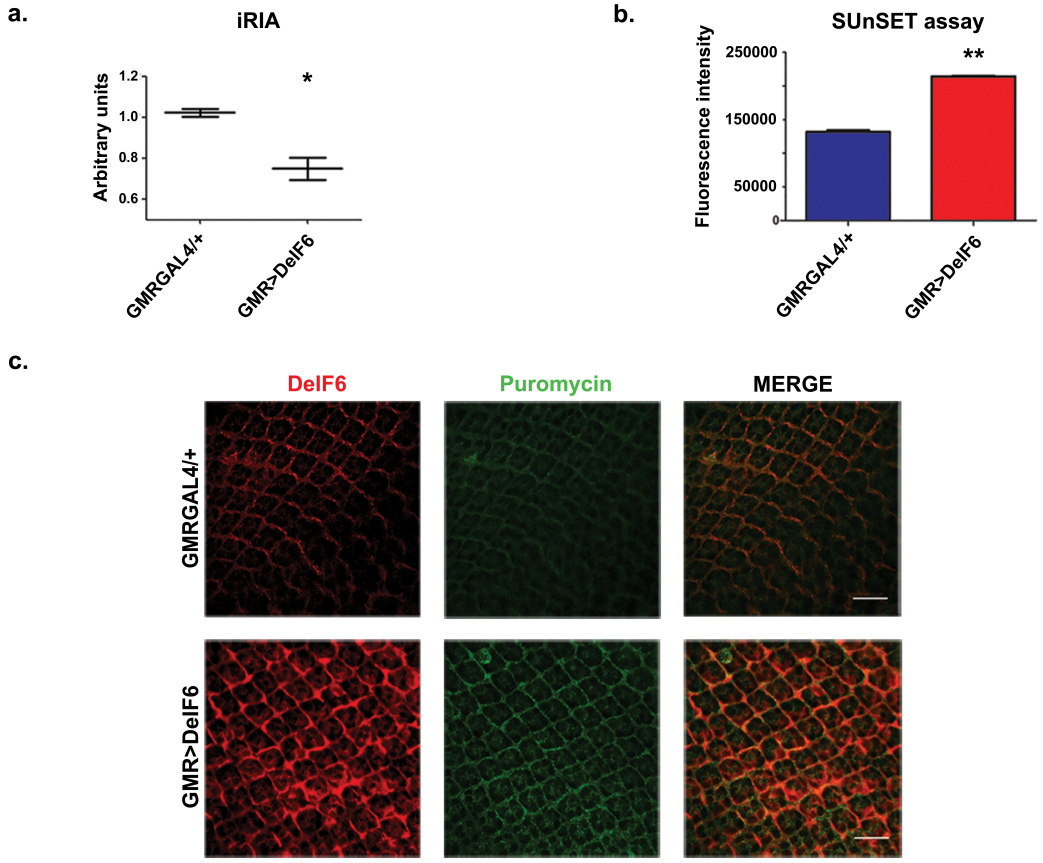

Figure 15: High levels of DeIF6 result in increased puromycin incorporation. a. iRIA assay demonstrates that ectopic expressed DeIF6 is able to bind the 60S. **b.** Quantification of SUnSET assay with ImageJ software. Graph represents mean ± SD. Statistic applied was *t-test*, paired, two tails. Experiments were performed at least three times. **c.** Representative immunofluorescence experiment of SUnSET assay, showing the two-fold increase in puromycin incorporation upon DeIF6 overexpression. Scale bar 10µm

to be expressed at this stage. We observed no differences neither in morphology nor in cell identities upon DeIF6 overexpression, when compared to control (Figure 17 a-c). More in details, we analyzed several markers in third larval instar eye imaginal discs: to identify neuronal cells we stained for ELAV, for cone cells we used Cut, while for R2/R5 photoreceptors we used Rough. All these cellular markers revealed no differences upon DeIF6 overexpression.

Next, we analyzed the effect(s) of DeIF6 overexpression in pupal development (Figure 18). Again, we stained for ELAV/Cut markers, finding that cells continued to

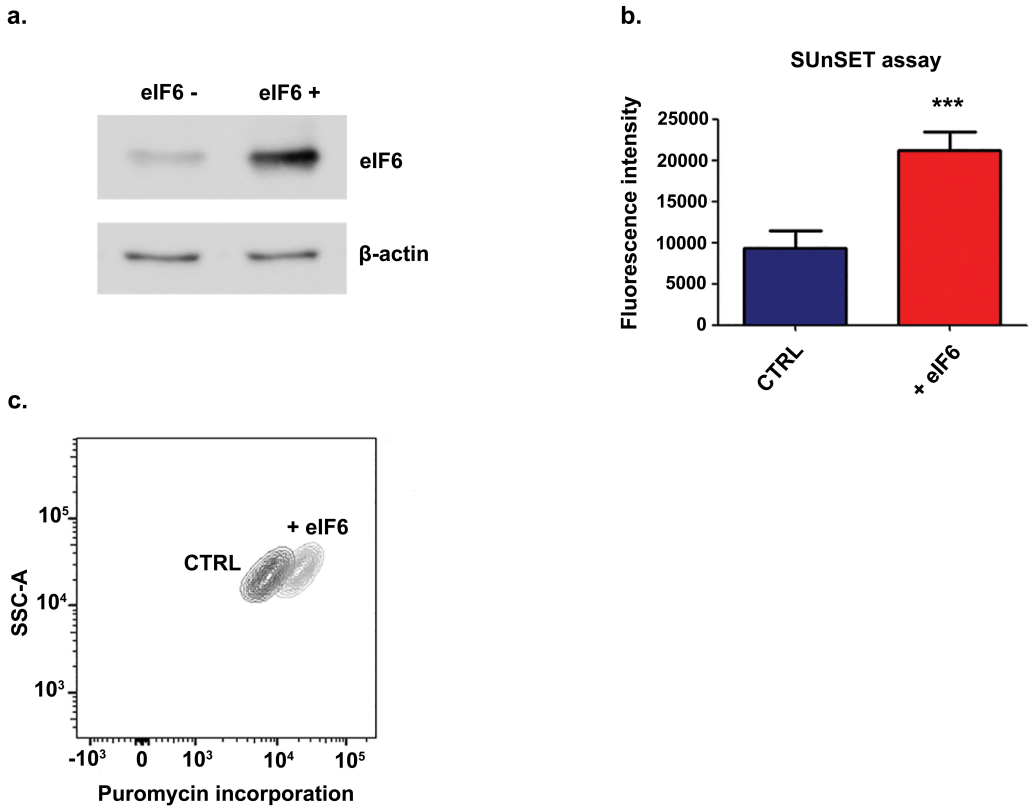

Figure 16: Increased puromycin incorporation driven by eIF6 overexpression is conserved also in mammalian cells. a. Representative western blot demonstrating eIF6 overexpression in HEK293 cells. **b.** Quantification of SUnSET assay with ImageJ software. Graph represents mean ± SD. Statistic applied was *t-test*, paired, two tails. Experiments were performed at least three times. **c.** Representative dot plot of citofluorimetry experiment of SUnSET assay in HEK293 cells showing overexpressing and control populations

maintain their identities and were present in the correct number, but their arrangment on the plane of the tissue was disrupted upon DeIF6 overexpression at 40 hours After Puparium Formation (APF) (Figure 18 b). To further confirm this phenotype, we also stained for another morphological marker, chaoptin, which localizes on the membranes of photoreceptors. We observed that *GMRGAL4/+* pupal retinae presented the typical pattern for chaoptin, showing all eight photoreceptors on a single plan, while DeIF6 overexpressing retinae did present all eight photereptorial cells, but never on the same focal plane (Figure 18 c). In addition to this intraommatidial defect, we also observed that ommatidia lost their neat columnar arrangement on

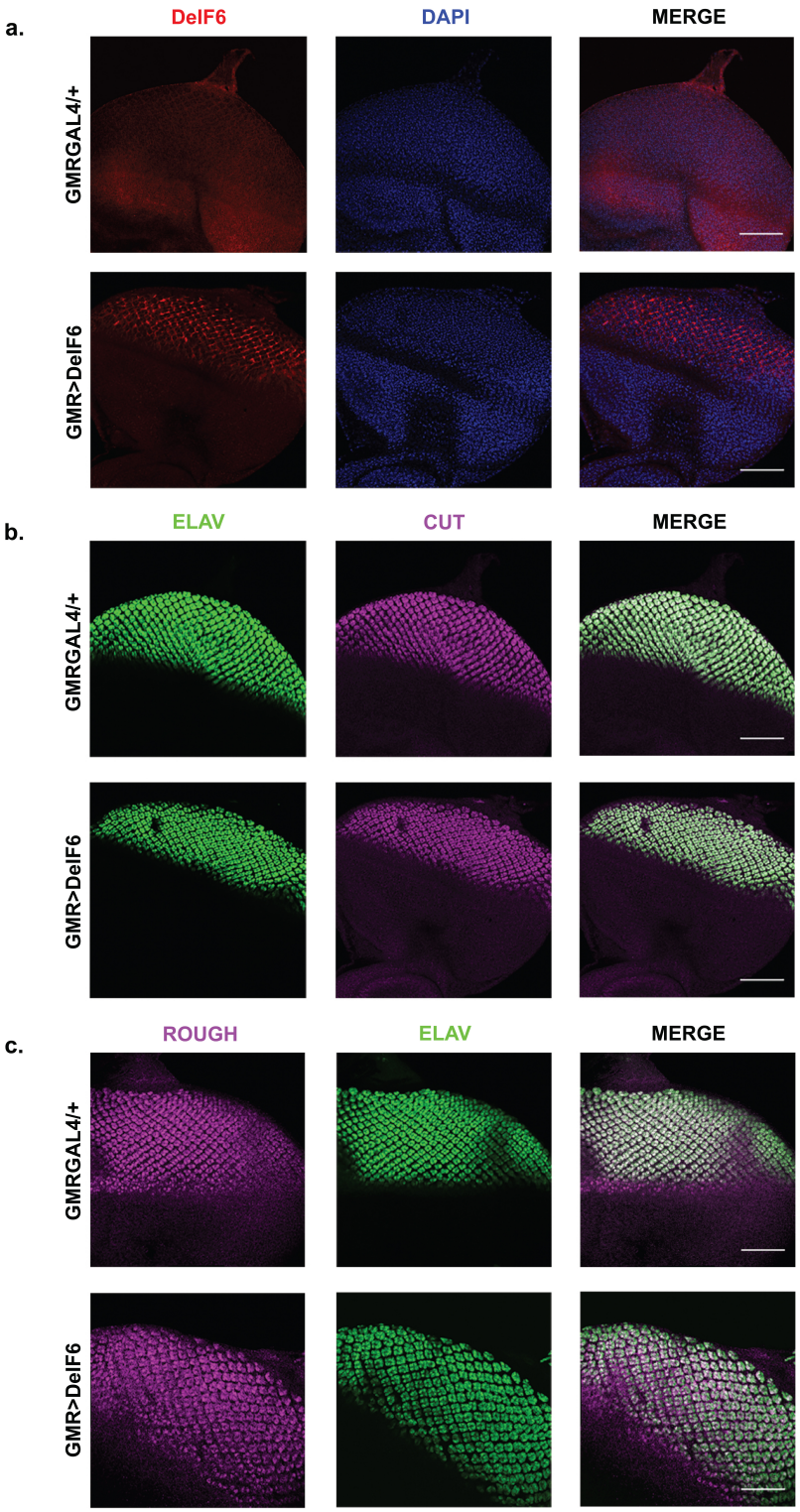

Figure 17: Cell identities and tissue morphology are preserved in larval eye imaginal discs upon DeIF6 overexpression. **a.** Immunofluorescence staining for DeIF6 to confirm the overexpression of the protein in the larval developmental stage. **b.** *GMRGAL4/+* and *GMR>DeIF6* eye imaginal discs stained for a neuronal (ELAV) and a cone (Cut) marker demonstrate that both cell types maintain their identity. **c.** Rough staining, specific fo R2/R5 photoreceptors, presents the same pattern for both *GMRGAL4/+* and *GMR>DeIF6*

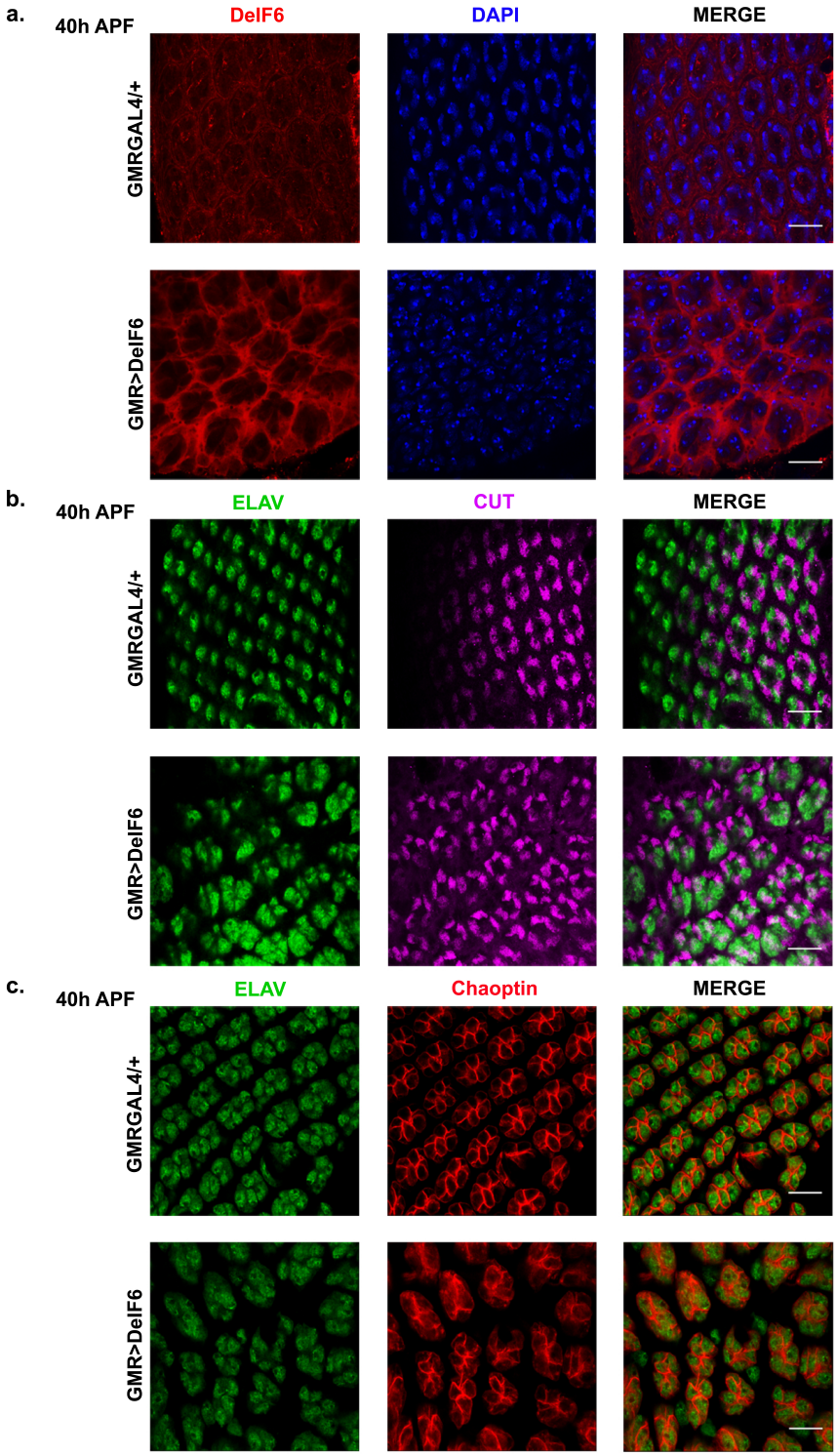

Figure 18: DeIF6 overexpressing mid-pupal retinae present aberrant morphology but preserved cell identities. a. Immunofluorescence staining for DeIF6 to confirm protein overexpression during pupal stage. **b.** *GMRGAL4/+* and *GMR>DeIF6* 40 hours APF retinae stained for ELAV and Cut demonstrate that both cell types maintain their identity but cells present an incorrect arrangment on the plane when DeIF6 levels are increased. **c.** Chaoptin staining, specific for intra-photoreceptors' membranes, show the aberrant intra- and interommatidial morphology associated with DeIF6 overexpression Scale bar 10 µm

the plane upon DeIF6 overexpression. Taken together, these morphological analyses strongly evidence that DeIF6 overexpression has no effect on cell identities, but rather disrupts their arrangement on the epithelial plane.

Among fundamental events that occur during pupal development and that control ommatidial morphology there is a wave of Programmed Cell Death (PCD), that sweeps the fly retina from 25 to 42 hours APF. We then decided to analyze PCD in our model. Interestingly, TUNEL assay performed at 28h APF showed that DeIF6 overexpressing retinae did not present apoptotic nuclei, conversely to control retinae (Figure 19 a).
The analysis of TUNEL (Figure 19 b) and of the *Drosophila* effector caspase, Dcp-1, at 40 hours APF (Figure 20 a), revealed again an intriguing absence of apoptotic cells in DeIF6 overexpressing retinae when compared to wild type ones. Interestingly, we observed Dcp-1 positive cells in *GMRDeIF6* retinae only later in development, at 60 hours APF (Figure 20 b). At this developmental time, wild type retinae did not show any Dcp-1 positive cell, confirming the end of the PCD in this developmental window. We quantified the number of Dcp-1 positive cells in both time points analyzed, revealing a striking 75% reduction at 40 hours APF in condition of high levels of DeIF6, and an 80% reduction at 60 hours APF (Figure 20 c).

We also performed another immunofluorescence experiment, by staining retinae with Armadillo, the *Drosophila* β-catenin homologue, that localizes on membranes of cells surrounding photoreceptors, thus giving an indication of their number. We found, at 40 hours APF, that *GMRGAL/+* retinae presented the expected Armadillo pattern, while DeIF6 overexpressing retinae showed the presence of extra-numerary cells around the ommatidial core (Figure 21 a, cells in excess indicated with $*$). We quantified the number of cells per ommatidium, finding that ommatidia of DeIF6 overexpressing retinae possessed 15 cells, roughly 30% more than their wild type counterpart (Figure 22 a). Conversely, at 60 and 72 hours APF, while *GMRGAL4/+* retinae continued to show the expected Armadillo pattern, the *Drosophila* β-catenin homologue was no longer detectable in DeIF6 overexpressing retinae (Figure 21 b

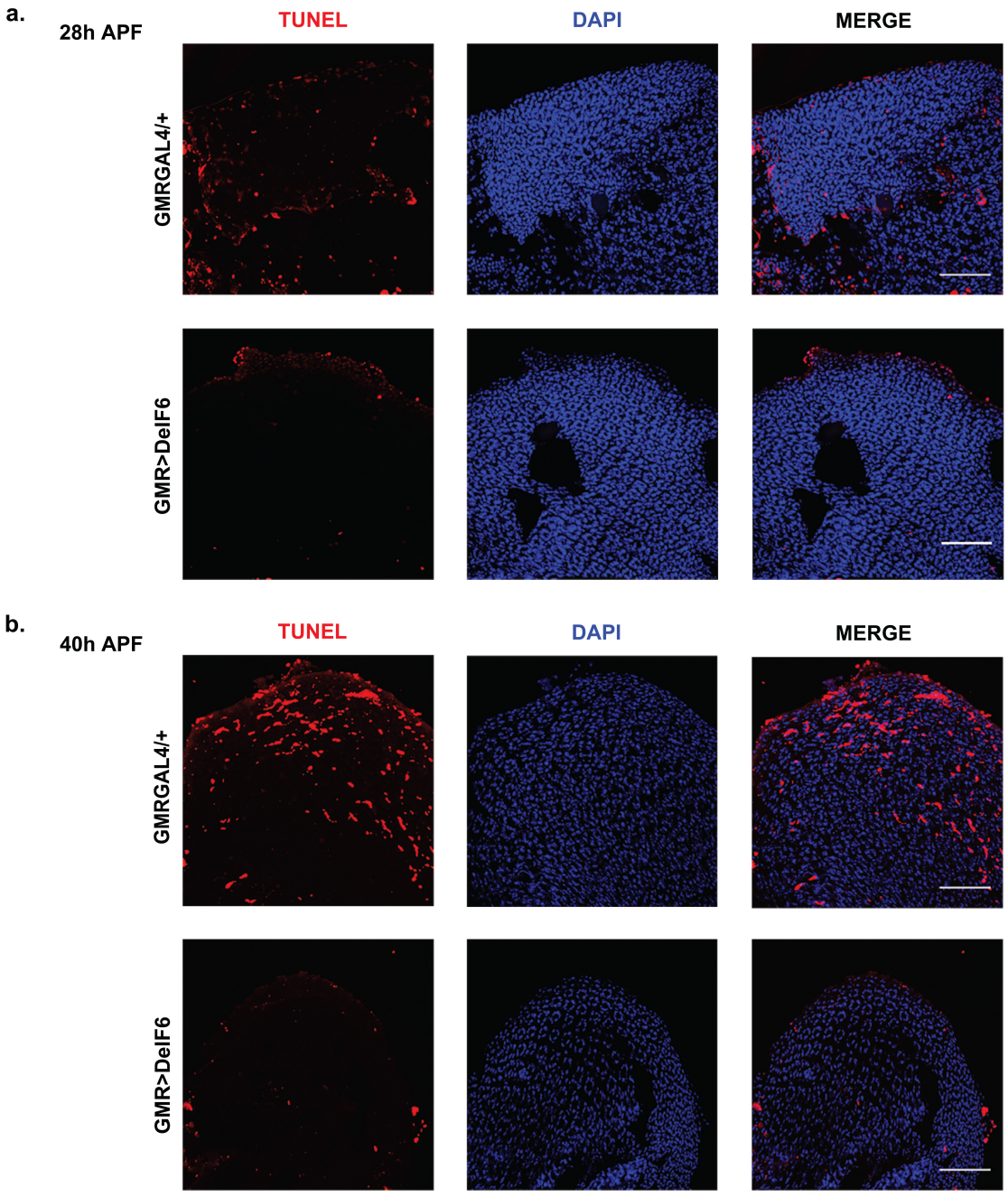

Figure 19: PCD is delayed when DeIF6 levels are higher than normal. TUNEL assay at 28 hours APF (**a.** and 40 hours APF **b.** in *GMRGAL4/+* and *GMR>DeIF6* show that PCD is blocked in these developmental stages upon DeIF6 overexpression. Scale bar 50 µm

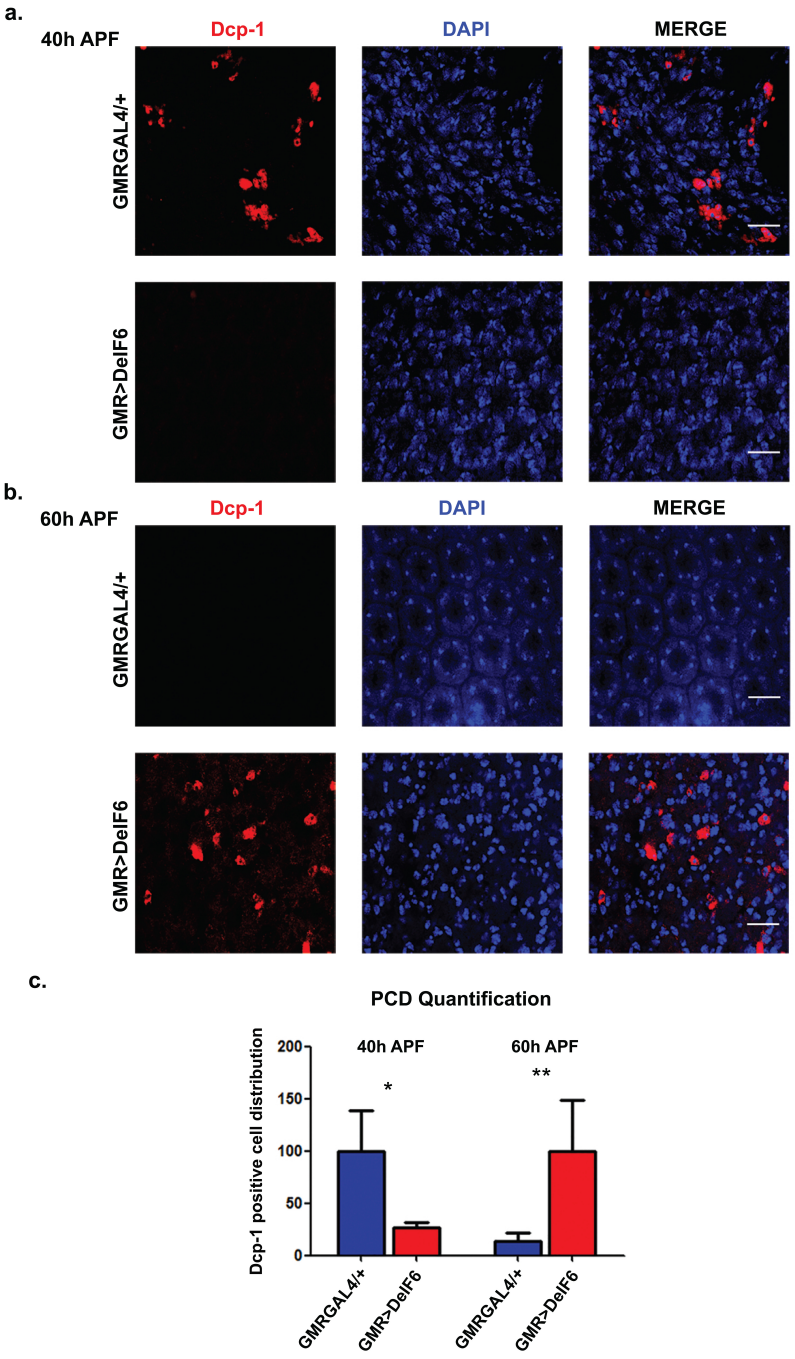

Figure 20: Increased *deif6* gene dosage results in delayed and increased PCD. **a.** Dcp-1 staining 40 hours APF. *GMRGAL4/+* presents Dcp-1 positive cells, i.e. dying cells, while *GMR>DeIF6* does not present any Dcp-1 positive cell, indicating a block in PCD **b.** 60 hours APF *GMRGAL4/+* retinae do not show any Dcp-1 positive cell, indicating that PCD is concluded at this developmental stage. Conversely, *GMR>DeIF6* retinae show Dcp-1 positive cells, indicating a delay of PCD. **c.** Quantification of Dcp-1 positive cells demostrates first a block and then an increase in the number of apoptotic cells upon DeIF6 overexpression. Scale bar 10 µm. Statistic applied was *t-test*, paired, two tails. Experiments were performed at least three times.

and 22 b). Then, with Armadillo staining we obtained another hint that PCD was first blocked and then aberrant upon DeIF6 overexpression. Taken together, these results demonstrate that the first effect of eIF6 overexpression is a strong delay in the onset of PCD, which might be the cause of the rough phenotype.

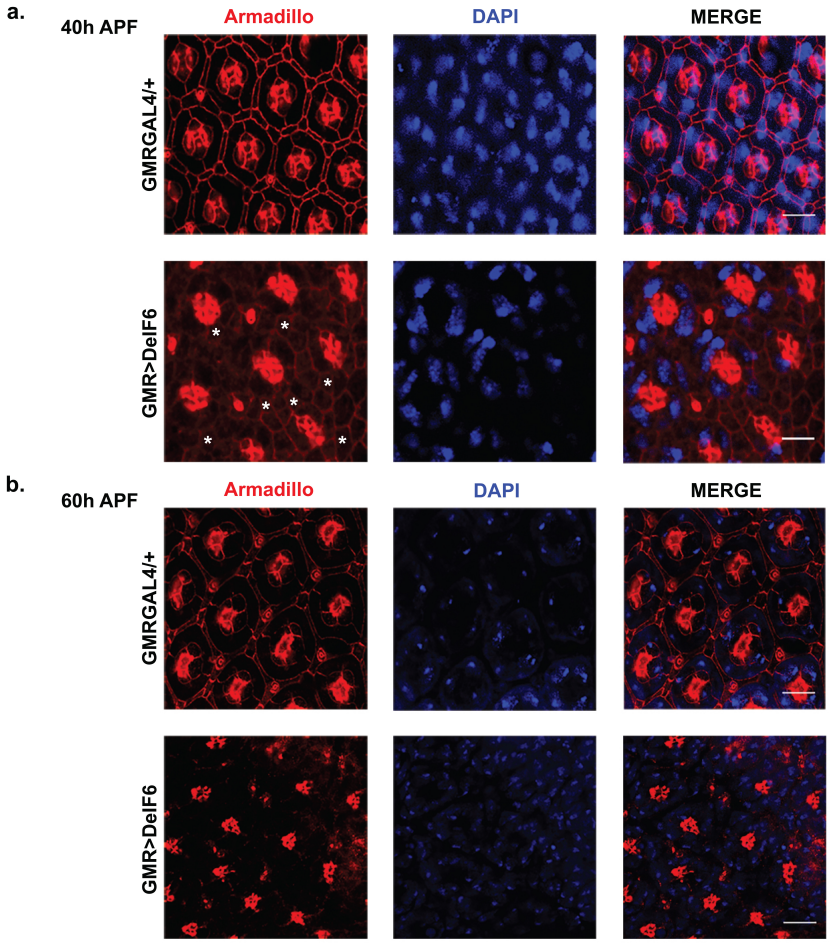

Figure 21: Cell number is altered when DeIF6 is overexpressed. a. 40 hours APF retinae stained for Armadillo, the *Drosophila* β-catenin homologue, showing the presence of extranumerary cells (indicated as $*$) when DeIF6 is overexpressed. **b.** 60 hours APF retinae stained for Armadillo. *GMRGAL4/+* retinae continue to present the expected pattern while *GMR>DeIF6* retinae show the loss of cells around ommatidia. Scale bar 10 µm.

a.

Genotype	Developmental stage	Cells per hexagon ± SD	Cells per ommatidium	Δ cells per ommatidium
GMRGAL4/+ (1)	40h APF	31.5 ± 0	10.5	-
GMRGAL4/+ (2)	40h APF	31.5 ± 0	10.5	-
GMR>DeIF6 (1)	40h APF	46 ± 2.8	15.3	+ 4.83
GMR>DeIF6 (2)	40h APF	39 ± 1.7	13	+ 2.5

b.

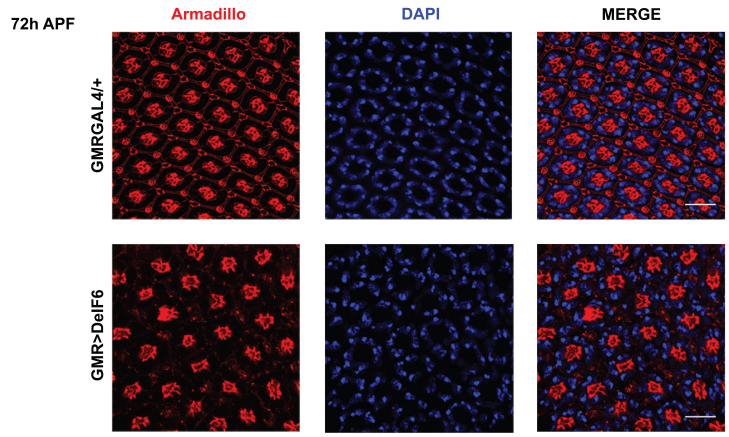

Figure 22: Alteration of cell number during pupal stage upon DeIF6 overexpression. a. Comparison of cell number around each ommatidium in the two genotypes, *GMRGAL4/* and *GMR>DeIF6*, showing an increase in *GMR>DeIF6* respect to control. **b.** Late pupal stage (72 hours APF) retinae stained for Armadillo show the loss of cells around ommatidia upon DeIF6 overexpression Scale bar 10 µm.

Overexpression of DeIF6 in specific cellular subtypes is sufficient to cause a *rough* eye through PCD alteration

PCD during pupal development is dependent on the crosstalk between two cell types: cone cells and Inter Ommatidial Cells (IOCs). Thus we overexpressed DeIF6 in either one of these two cell types, with the *spaGAL4* or *54CGAL4* drivers respectively. The overexpression here resulted in a *rough* eye phenotype, albeit milder with respect with the one obtained with the *GMRGAL4* driver (Figure 23).

We then characterized *spaGAL4* rough eye, and we observed, with tangential semithin sections, that also with this driver the structure of the compound eye was lost but photoreceptors were present and in the correct number (Figure 24 a).

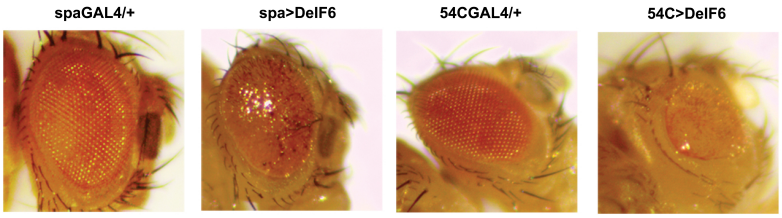

Figure 23: Increasing *deif6* gene dosage specifically in cone and interommatidial cells is sufficient to cause a rough phenotype. Stereomicroscope images of *spa>DeIF6* and *54C>DeIF6* eyes, showing that the overexpression of DeIF6 only in cone and interommatidial cells repectively is sufficient to cause in a *rough* phenotype.

Analyzing pupal development, we observed the neat DeIF6 overexpression only in cone cells (Figure 24 b), and again the disrupment of the arrangement of cells on the plan even though their identities were maintained (Figure 24 c). Moreover, we confirmed the absence of Dcp-1 positive cells upon DeIF6 overexpression restricted in cone cells, when compared to control at 40 hours APF (Figure 25 a). Dcp-1 apoptotic nuclei were instead present at 60 hours APF in cone cell DeIF6 overexpressing retinae, in the same temporal pattern presented by *GMRGAL4* overexpressing retinae (Figure 25 b). To further confirm that PCD was responsible for the rough eye observed when overexpressing DeIF6 in all cells of the eye, or only in cone cells or IOCs, we blocked apoptosis by co-expressing DeIF6 with the Baculovirus caspase inhibitor p35, under the control of the *GMRGAL4* driver. Intriguingly, we observed an almost complete rescue of the rough eye (Figure 26). Taken together, these data suggest that altered PCD is likely responsible for the rough eye phenotype.

Developmental defects associated with increased DeIF6 levels are not tissue specific

Once determined that DeIF6 overexpression in the eye correlated with increased general translation and delayed PCD, we asked whether such defects were organ specific or a more general effect of DeIF6 high levels. To answer this question, we took

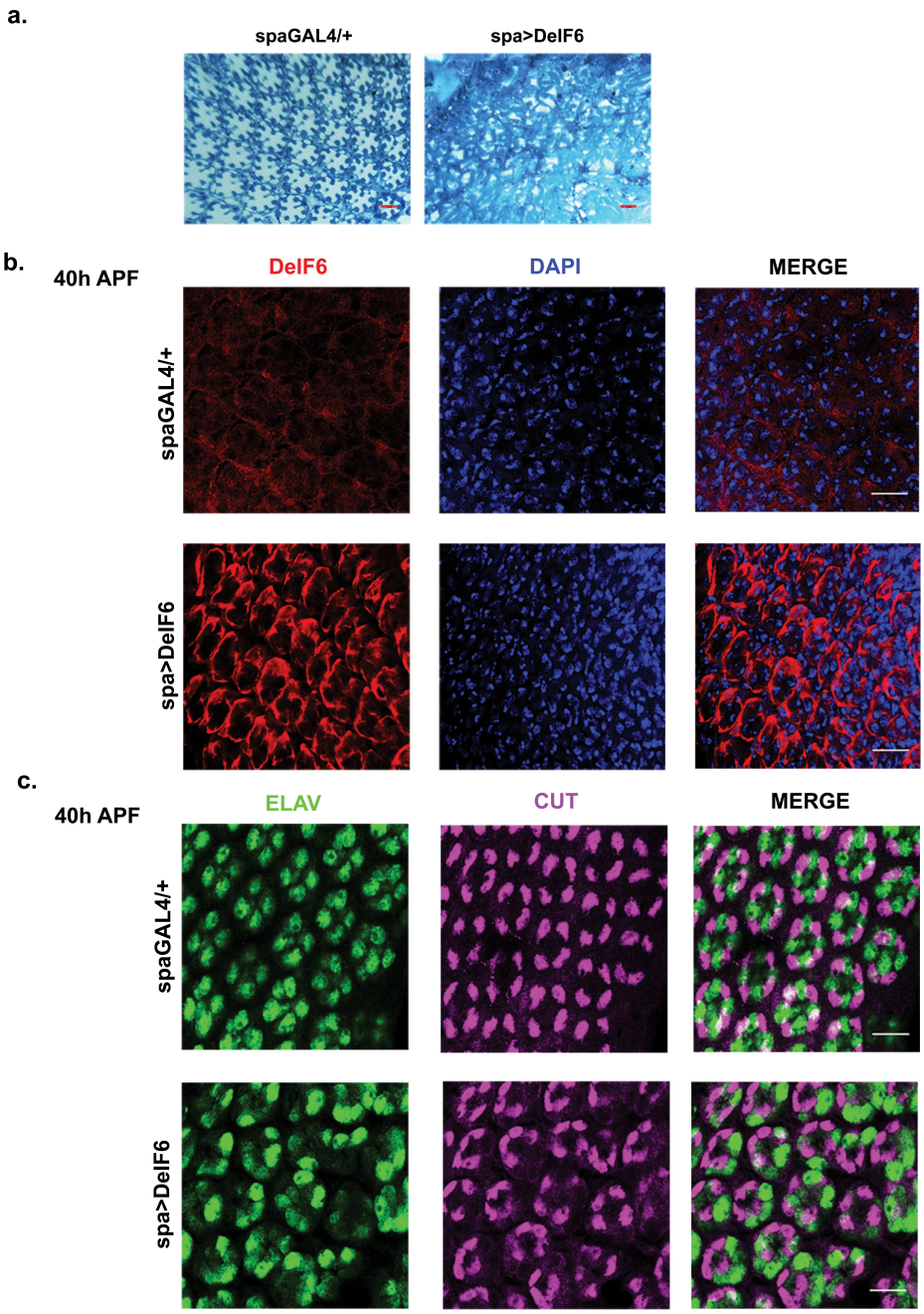

Figure 24: Characterization of rough phenotype of *spa>DeIF6* flies. **a.** Representative tangential sections of *spaGAL4/+* and *spa>DeIF6* showing the disrupted structure upon DeIF6 specific overexpression in cone cells. **b.** Mid-pupal retinae stained for eIF6 to confirm that overexpression of the protein is restricted to cone cells. **c.** Mid pupal stage retinae stained for ELAV and Cut confirm that neuronal and cone cells identities are maintained but their arrangement on the plane is lost.

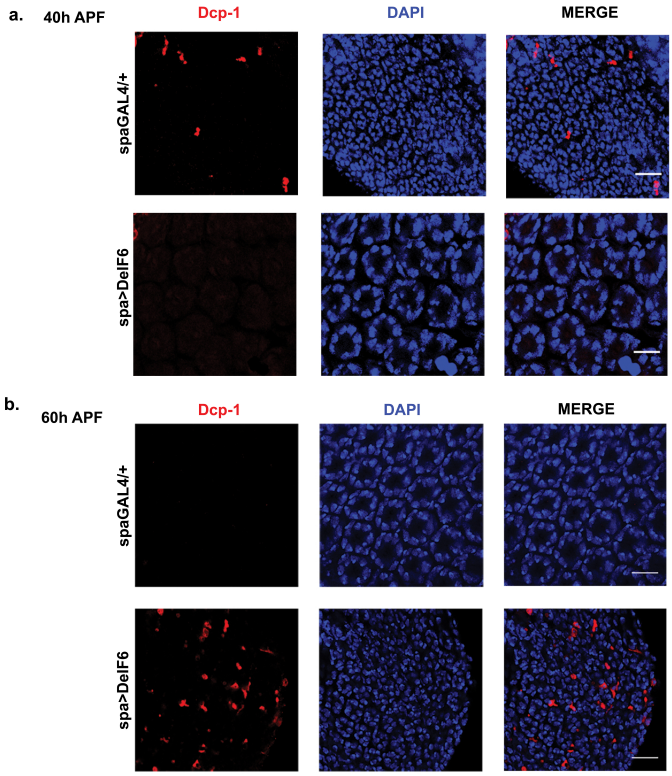

Figure 25: ***spa>DeIF6*** **presents the same apoptotic defect of** ***GMR>DeIF6.*** **a.** Dcp-1 staining 40 hours APF. *spaGAL4/+* presents Dcp-1 positive cells, i.e. dying cells, while *spa>DeIF6* does not present any Dcp-1 positive cell, exactly as *GMR>DeIF6* mid-pupal retinae. **b.** 60 hours APF *spaGAL4/+* retinae do not show any Dcp-1 positive cell, indicating that PCD is concluded at this developmental stage. Conversely, *spa>DeIF6* retinae show Dcp-1 positive cells, indicating a delay of PCD

advantage of another *Drosophila* driver, the *MSGAL4*, which overexpresses its UAS target only in the dorsal wing disc. We observed that the wings overexpressing DeIF6 presented a completely shattered structure (Figure 27 a). In addition, SUnSET assay on wing imaginal discs revealed again a two-fold increase in puromycin incorporation upon DeIF6 overexpression (Figure 27 b-c). We also observed a dramatic increase in Dcp-1 positive cells, i.e. cells undergoing apoptosis, in the dorsal portion of the wing imaginal disc, specifically where DeIF6 is overexpressed (Figure 27 d). Taken together, these results indicate that DeIF6 increased levels are detrimental in developing tissues by a pronounced increase in both general translation and apoptosis.

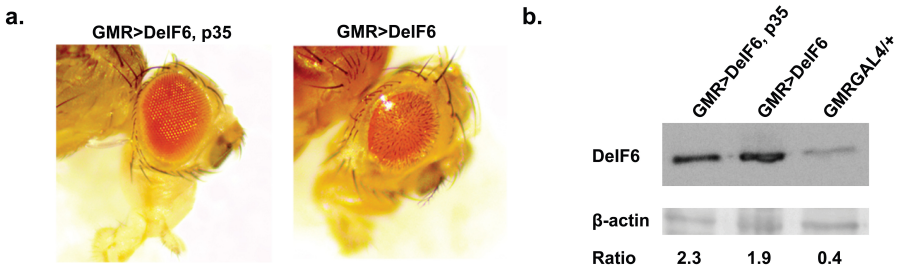

Figure 26: Apoptosis is responsible of the rough phenotype. a. Representative stereomicroscope images of *GMR>DeIF6;p35* and *GMR>DeIF6* adult eyes. **b.** Western blot of DeIF6 levels in *GMR>DeIF6;p35* and *GMR>DeIF6*. For each genotype, densitometric ratio (DeIF6/β-catenin) was calculated with ImageJ.

Gene expression analyses reveal a transcriptome rewiring that results in altered ribosome maturation and ecdysone signalling

We assessed that increased *DeIF6* gene dosage resulted in increased translation and apoptosis, in a tissue unspecific manner. We then asked if *DeIF6* increased gene dosage was also able to induce transcriptional changes. To this end, we performed two indipendent RNASeq experiments, by comparing eye imaginal discs and 40 hours APF pupal retinae of *GMRGAL4* and *GMR>DeIF6* genotypes (Figure 28).

Interestingly, we observed, in both developmental windows analyzed, a common trend for several gene sets, including a common upregulation of genes related to ribosome biogenesis upon DeIF6 overexpression (Figure 28 a). Strikingly, our GSAA analysis revealed that also the rRNA processing subsets were upregulated. These observation strongly point to a role of ribosome biogenesis inducer for eIF6. In our gene expression analysis we also found confirmation to our experimental conclusions: indeed, we found an upregulation of genes related to apoptosis and PCD in our overexpressing pupal samples (Figure 28 a,c). On the other hand, mRNAs encoding specialized eye enzymes, such the ones responsible for pigments biosynthetic pathways, were downregulated upon DeIF6 overexpression. These observations were consistent with altered eye morphology. Intriguingly, the most changed genes associated with

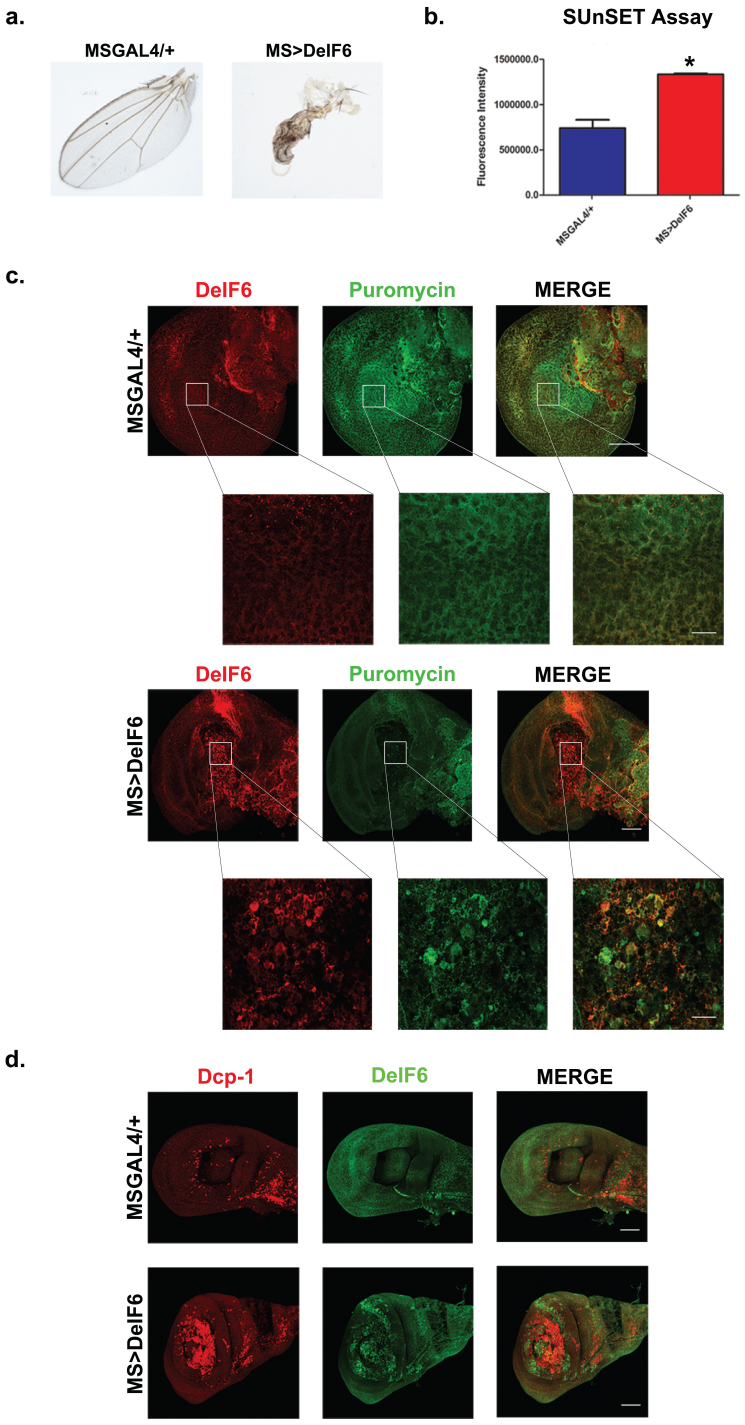

Figure 27: Developmental defects induced by *deif6* increased gene dosage are not tissue specific. a. Representative stereomicroscope images of *MSGAL4/+* and *MS>DeIF6* adult wings, showing the complete shuttered structure of the wing overexpressing DeIF6. **b.** SUnSET assay quantification by ImageJ show a two-fold increase in puromycin incorporation upon DeIF6 overexpression in wing imaginal discs, consistent with results obtained in eye imaginal discs. Graph represents mean ± SD. Statistic applied was *t-test*, paired, two tails. Experiment was performed at least three times. **c.** Representative SUnSET assay performed through immunofluorescence, indicating the two-fold increase in puromycin incorporation. For each genotype, two magnifications are compared: 63x (scale bar 50 µm) and 252x (scale bar 10 µm). **d.** Apoptosis is increased in wng imaginal discs overexpressing DeIF6. Wing imaginal discs stained for Dcp-1 and DeIF6 in control (*MSGAL4/+*) and DeIF6 overexpressing imaginal wings (*MS>DeIF6*) showing the striking increase of apoptotic cells upon DeIF6 overexpression.

DeIF6 overexpression all belonged to one specific pathway, the ecdysone pathway. Indeed, when DeIF6 was overexpressed we found a striking downregulation of many genes involved in the biosynthesis of the steroid hormone active form, 20-HydroxyEcdysone (20-HE). For example, we found that *nvd, phm* and *sad* were almost absent in DeIF6 larval overexpressing samples, and also genes belonging to the early (*rbp*) and late (*ptp52f*) ecdysone signalling cascade were downregulated as well (Figure 28 a-b). Thus, we can conclude that DeIF6 overexpression leads to an overall silencing of the ecdysone pathway. In addition, we found that gene sets related to chromosome organization were upregulated in *GMR>DeIF6* samples, suggesting a possible role of the initiation factor on epigenetics. For this reason, we analyzed the enzymatic activity of Histone Deacetylases (HDACs), which remove acetyl groups from histones. We found an interesting two-fold decrease of HDACs activity (Figure 28 d) when analyzing DeIF6 overexpressing adult eyes, compared to control. Interestingly, it has already been demonstrated that transcription of ecdysone biosynthetic enzymes is strictly under the control of epigenetics. Overall, our data provide a potential causal link between translation and control of transcription, demonstrating that overexpression of DeIF6 correlates with silencing of ecdysone signalling and reduction of HDACs activity.

Ecdysone administration partially rescues the adult phenotype

Gene expression analysis strongly pointed to a silencing of ecdysone signalling upon DeIF6 overexpression. Thus, we asked whether the shutdown of this hormonal pathway could be responsible for the observed *GMR>DeIF6* phenotype. To address this issue, we administered 20-HE to third instar larvae, and analyzed apoptosis at 40 hour APF and adult morphology. Strikingly, we observed that 20-HE administration led to a partial rescue of the apoptotic defect. Indeed, staining for Dcp-1 at 40 hours APF showed the precence of apoptotic cells in *GMR>DeIF6* retinae treated with

the active form of the hormone, which were instead absent in not treated DeIF6 overexpressing control (Figure 29 a). Consistently, also adult eyes of *GMR>DeIF6* treated with 20-HE showed a partial rescue of the rough phenotype (Figure 29 b). More in detail, upon DeIF6 overexpression eyes were 30% smaller than control. Instead, when treated with the hormone, the adult eye observed was 20% larger than untreated control, even if still rough and smaller than *GMRGAL4/+* eyes. These data strongly indicate that the overall reduction in ecdysone signalling causes the apoptotic and morphological defects observed upon DeIF6 overexpression.

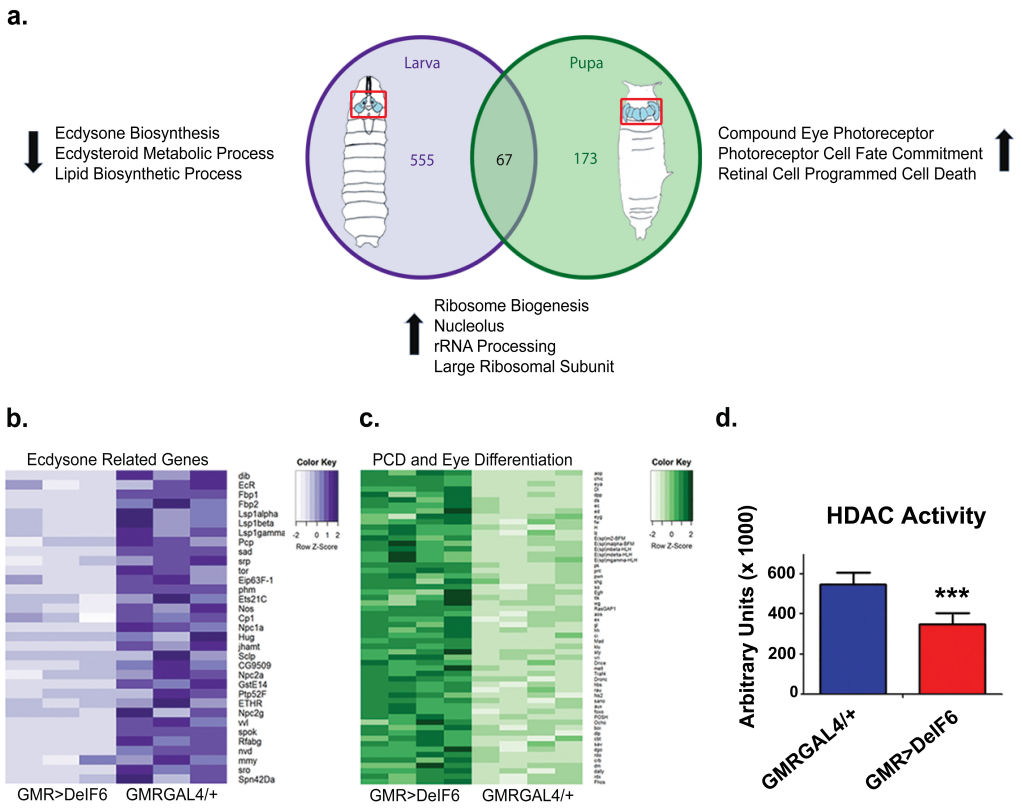

Figure 28: Gene expression analyses show a transcriptional rewiring and the downregulation of ecdysone pathway. a. Venn diagram showing genes differentially expressed in *GMR>DeIF6* eye imaginal discs and mid-pupal stage retinae respect to control (*GMRGAL4/+*). **b.** Heat Map representing absolute gene expression levels in *GMR>DeIF6* and *GMRGAL4/+* eye imaginal disc samples for the gene set of ecdysone biosynthesis by Gene Ontology, showing the striking shut off the ecdysone biosynthetic pathway upon DeIF6 overexpression. **c.** Heat Map representing absolute gene expression levels in *GMR>DeIF6* and *GMRGAL4/+*for the subset of genes involved in PCD and Eye Developmnet in pupal samples, showing the upregulation of these genes upon DeIF6 overexpression. **d.** Representative graph showing lower HDACs activity in association with high DeIF6 protein levels. The assay has been performed on adult heads protein extracts.

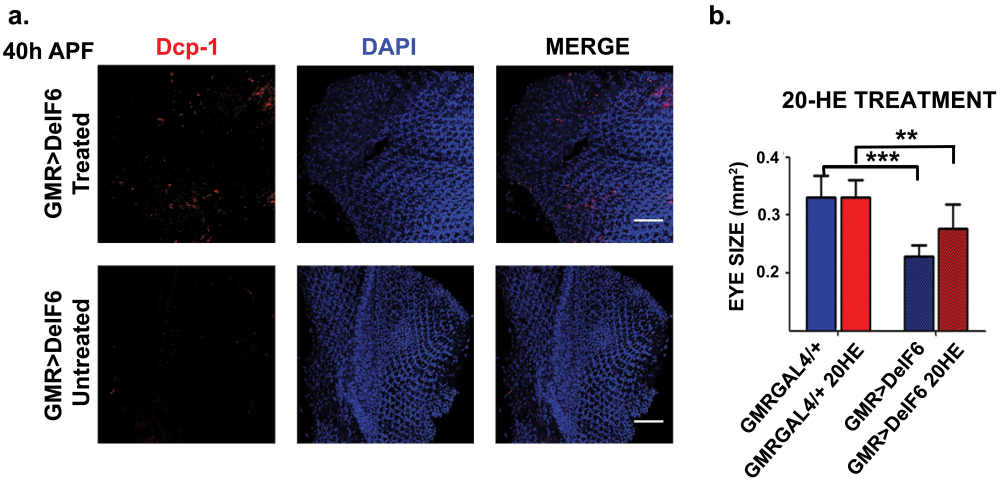

Figure 29: 20-Hydroxy-Ecdysone treatment partially rescues rough phenotype. **a.** immunofluorescence images showing that treating with 20-HE partially rescues the apoptotic defect observed in *GMR>DeIF6* 40 hours APF retinae. **b.** Representative graph showing the adult fly size with or without 20-HE treatment. The reduced fly eye size associated with *GMR>DeIF6* genotype is partially rescue after 20-HE treatment. Graph represents mean ± SD. Statistic used was *t-test*, two tails, paired. Experiment was repeated at least three times.

Discussion

Here, we present the first *in vivo* model of *eif6* increased gene dosage, using *Drosophila* eye. Our starting point was the knowledge that eIF6 is upregulated or hyperphosphorylated in several cancer types, and that *eif6* locus is amplified in luminal breast cancer, but the early effects of this upregulation are still unclear. We demonstrate that higher levels of eIF6, which is a factor necessary for ribosome biogenesis and translation, are sufficient to induce an increase in ribosome biogenesis and general translation that generates a complex transcriptional and metabolic reprogramming. This in turn blocks apoptosis and causes the shutoff of hormonal production (Figure 30). Rescue of hormonal supply partly reverts apoptosis and the related developmental deficits, demonstrating that translation acts upstream of transcription and metabolism *in vivo*.

Specifically, we show that a modulation of eIF6 expression during development or in the whole organism is incompatible with life. The *Drosophila* DeIF6 shares 90% of similarity with its human homologue. We decided to take advantage of the fly model and its genetic tools [131] to modulate DeIF6 gene dosage *in vivo* and analyze the early effects of eIF6 increased levels. To avoid the viability issue of the intact organism, we increased DeIF6 levels only in the fly eye, a dispensable organ, that is widely used for its well known structure and development [132]. Intriguingly, upon DeIF6 overexpression we observed a rough eye phenotype, that we deeply characterized during development. We demonstrated three major features associated with increased DeIF6 protein levels: an increase in general translation, a delayed and aberrant apoptosis and a total shutdown of the ecdysone hormonal pathway.

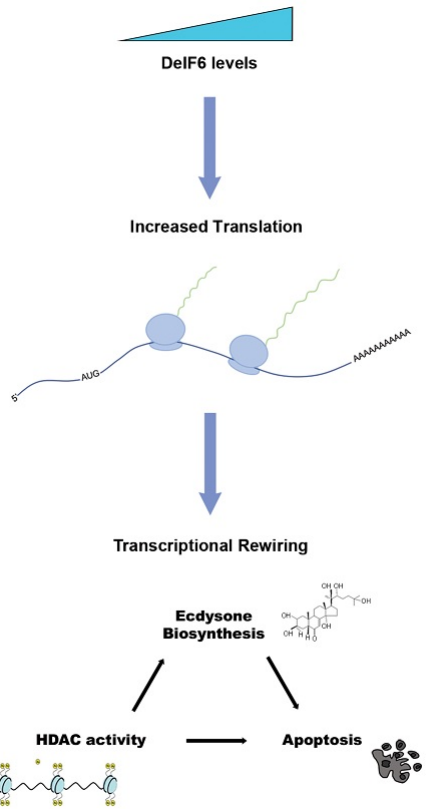

Figure 30: Model for DeIF6 high levels-associated changes. We demonstrated that increased levels of DeIF6 are associated to increased general translation, resulting in a transcription rewiring. RNASeq analysis confirms that altering deif6 gene dosage modulates apoptosis during development and interestingly, reveals a shutdown of genes involved in 20-HydroxyEcdysone biosynthesis. In addition, we found an upregulation of genes related to chromatin organization.

We will discuss them separately.

In recent years, many studies have highlighted how alterations in the ribosomal machinery and/or in translational control are involved in several pathologies, [133]. Indeed, increased expression of some ribosomal proteins (RPs) and of eukaryotic Initiation Factors (eIFs) has been found in many cancer types [134–136]. Increased protein synthesis was often interpreted as a general by-product of increased proliferation. Recently, instead, it has become evident that deregulation of the translational machinery can be causative of cancer. Translation is the most energy consuming process in cells [9]. For this reason, translation is tightly regulated, mostly in its initiation step. The eukaryotic initiation factor eIF6, which is essential for both ribosome biogenesis and translation initiation [23, 42], was found upregulated in

many cancer types, including breast cancer, colorectal cancer and mesothelioma [40, 41, 45]. Consistently, haploinsufficiency of eIF6 protects mice from lymphomagenesis in an Eμ-Myc model [43]. eIF6 acts by increasing the translational capability of cells upon growth factor stimulation. eIF6 is an essential player in the control of initiation of translation, because of the need to release it from the 60S for the joining of the two ribosomal subunits and the following initiation of translation [23, 137]. In our eIF6 overexpressing model, we observed an unexpected increase in mRNAs encoding for ribosomal proteins and rRNA processing factors, suggesting that ribosome biogenesis is upregulated when eIF6 levels are higher than normal. Interestingly, we also showed that the overexpression of DeIF6 causes a two-fold increase of general translation, measured as puromycin incorporation, both in the developing eye and wing. This new mechanistic effect extends the previous observation that demonstrated the role of eIF6 in the translation of uORFs containing mRNAs [44, 138]. These data, taken together, show that eIF6 can act in a feed-forward loop that amplifies the efficiency of the translational machinery, and suggest that the upregulation of eIF6 may give advantage to cancer cells, through an upregulation of both ribosome biogenesis and general translation, both necessary to sustain the high proliferative rate of malignant cells.

It is also possible that an increase in general translation such as the one dictated by excess eIF6 impacts tumour cell fate in other ways, beyond the immediate necessity of an augmented protein synthesis. A possible answer to this is represented by the inhibition of physiological PCD in the fly eye during the pupal stage [105] upon DeIF6 overexpression. A similar observation was made in *X. laevis* [139]. The deregulation of PCD is in itself responsible for the rough eye phenotype observed in condition of increased DeIF6 levels. In addition to this observation, here we defined a molecular array of events that precedes and follows the inhibition of apoptosis. By high-throughput gene expression analyses we found that an upregulation of general translation causes a gross change in the transcriptome that has a coordinated impact in biological processes, including apoptosis. We performed two independent gene

expression analyses, in two distinct developmental windows: the first in the larva, to appreciate the early events associated to DeIF6 overexpression, the latter in mid pupal stage, when we experimentally observed the apoptotic defect. Interestingly, in this last gene expression experiment, performed when the apoptotic wave shapes the fly retina eliminating extra-numerary cells, we observed a global up-regulation of genes involved in apoptosis. Overall, the effects of the manipulation of a translation factor resulted in a change in apoptosis that is therefore explained by transcriptional changes. This observation means that protein synthesis can acquire a driver role in transcription, a feature stil under appreciated in molecular biology. In summary, our data on apoptosis are consistent with two possibilities: developmental PCD could be delayed by excess DeIF6. Alternatively, PCD could be repressed at the correct developmental time and apoptotic elimination of defective cells overexpressing DeIF6 could be triggered later independently of developmental signals. The fact that overexpression of DeIF6 in wing discs, which are not subjected to developmental apoptosis, leads to cell death supports the latter hypothesis. Overall, these considerations indicate that the advantage provided by excess DeIF6 to tumour cells might initially consist in escape from apoptotic clearance. The following increase in apoptosis that we observed later in development, at 60 hours APF, could be dependent on an organ failure caused by the inability to remove excess cells. On the contrary, tumors are not affected by this issue because they are not functional organs, but parasitic structures.

Gene expression analysis performed in the larvae strongly points to a total shutdown of ecdysone biosynthesis and signaling. In our analysis, almost all of the mRNAs of the ecdysone biosynthetic pathway are greatly transcriptionally downregulated, some of them even completely turned off, and the ecdysone signaling pathway is globally affected upon DeIF6 overexpression. In addition, 20-HE treatment led to a partial rescue of the pupal apoptotic defect and therefore of the rough eye phenotype. Indeed, upon 20-HE treatment, we observed the partial rescue of PCD at 40 hours APF and also the resulting adult eye presented a milder phenotype

respect to not treated *GMR>DeIF6* eyes. It is worth to note that the treatment with the steroid hormone could only be an acute one: we could only treat larvae, but upon pupariation and subsequent metamorphosis into adults, the developing flies do not eat the flyfood containing the hormone. Therefore, it is possible that a more continous treatment would result in a complete rescue of the phenotype. This issue needs to be further covered in future experiments. Nonetheless, our data place DeIF6 upstream of ecdysone regulation, that is in turn responsible for the incapability of DeIF6 overexpressing retinae to undergo apoptosis in the right developmental window.

It has been established that epigenetic changes control the transcription of ecdysone biosynthetic enzymes [140, 141]. We previously found that, in mammals, eIF6 haploinsufficiency caused a puzzling signature that mimicked alterations obtained by histones acetylation inhibitors [44]. Intriguingly, our larval GSAA analysis unveils that genes belonging to the chromosome organization gene set, such as Gcn5 and Ada1-2, are upregulated when DeIF6 is overexpressed. Here, we showed that eIF6 expression leads to a decrease in HDACs activity. Overall, these data suggest that DeIF6 overexpression causes a transcriptional reshaping that leads to complex epigenetic changes which in turn prevent the transcription of mRNAs of the ecdysone biosynthetic pathway. Curiously, an HTS screening for modulators of chromatin structure, years ago identified as a major player another initiation factor [142].

Globally, these data bring translation to a center stage in the global regulation of gene expression, at multiple levels. In summary, our study discloses for the first time a regulation of a hormonal biosynthetic pathway dependent on an eukaryotic translation factor that may act upstream of global and metabolic transcriptional rewirings. The *Drosophila* model that we have established and presented here, may be also used for an *in vivo* screening of suppressors of eIF6 overexpression that can be useful in cancer therapy in view of the strong protumorigenic role of mammalian eIF6.

Materials and Methods

Genetics

Fly strains were maintained on standard cornmeal food at 18°C. Genetic crosses were performed at 25°C, with the exception of GMRGAL/+ and GMR>deIF6, performed at 18°C. The following fly mutant stocks have been used: GMRGAL4/CTG was a gift from Manolis Fanto (King's College, London); UAS-DeIF6 was a gift from William J Brook (Alberta Children's Hospital, Calgary) [143]. Lines obtained from the Bloomington Drosophila Stock Center (BDSC): spaGAL4 (26656), 54CGAL4 (27328) and w1118, UAS-p35 (5072), UAS-mCD8GFP (32184), MSGAL4 (8860).

Cell culture and transfections

HEK293T cells were grown in DMEM (Lonza) supplemented with 10% Fetal Bovine Serum (FBS) and 1% penicillin, streptomycin, L-glutamine (Gibco) and maintained at 37°C and 5% CO_2. Mycoplasma testing was performed before experiments. Cells were transfected with pcDNA3.1-eIF6 [29], or an empty vector, with Lipofectamine®2000 (Invitrogen # 11668019) following manufacturer protocol.

RNA isolation and RNA sequencing

Total RNA was extracted with mirVanaTM isolation kit according to the manufacturer protocols (mirVana ThermoFisher # AM 1560) from 10 eye imaginal discs (larval stage) or 10 retinae (pupal stage). RNA quality was controlled with BioAnalyzer. Libraries for Illumina sequencing were constructed from 100 ng of total RNA with the Illumina TruSeq RNA Sample Preparation Kit v2 (Set A). The generated libraries were loaded on to the cBot (Illumina) for clustering on a HiSeq Flow Cell v3. The flow cell was then sequenced using a HiScanSQ (Illumina). A

paired-end (2×101) run was performed using the SBS Kit v3 (Illumina). Sequence deepness was at 35 millions reads.

Bioinformatic Analysis

Read pre-processing and mapping

Three biological replicates were analyzed for GMRGAL4/+ and GMR>DeIF6 larval eye imaginal discs and four biological replicates were analyzed for GMR-GAL4/+ and GMR>DeIF6 pupal retinae, for a total of 14 samples. Raw reads were checked for quality by FastQC software (version 0.11.2, S., A.FastQC: a quality control tool for high throughput sequence data. 2010; Available from: http://www.bioinformatics.babraham.ac.uk/projects/fastqc), and filtered to remove low quality calls by Trimmomatic (version 0.32) [144] using default parameters and specifying a minimum length of 50. Processed reads were then aligned to *Drosophila* melanogaster genome assembly GRCm38 (Ensembl version 79) with STAR software (version 2.4.1c) [145].

Gene expression quantification and differential expression analysis.

HTSeq-count algorithm (version 0.6.1, option -s = no, gene annotation release 79 from Ensembl) [146] was employed to produce gene counts for each sample. To estimate differential expression, the matrix of gene counts produced by HTSeq was analyzed by DESeq2 [147]. The differential expression analysis by DeSeq2 algorithm was performed on the entire dataset composed by both larvae and pupae samples. The two following comparisons were analyzed: GMR>DeIF6 versus GMRGAL4/+ larval eye imaginal discs (6 samples overall) and GMR>DeIF6 versus GMRGAL4/+ pupal retinae (8 samples in total). Reads counts were normalized by calculating a size factor, as implemented in DESeq2. Independent filtering procedure was then applied, setting the threshold to the 62 percentile; 10886 genes were therefore tested for differential expression. Significantly modulated genes in GMR>DeIF6 genotype were selected by considering a false discovery rate lower than 5%. Regularized logarithmic (rlog) transformed values were used for heat map representation of gene expression profiles. Analyses were performed in R version 3.3.1 (2016-06-21,

Computing, T.R.F.f.S. R: A Language and Environment for Statistical Computing. Available from: http://www.R-project.org/).

Functional analysis by topGO

The Gene Ontology enrichment analysis was performed using topGO R Bioconductor package. The option nodesize = 5 is used to prune the GO hierarchy from the terms which have less than 5 annotated genes and the annFUN.db function is used to extract the gene-to-GO mappings from the genome wide annotation library org.Dm.eg.db for *D. melanogaster*. The statistical enrichment of GO was tested using the Fisher's exact test. Both the "classic" and "elim" algorithms were used.

Gene set association analysis

Gene set association analysis for larvae and pupae samples was performed by GSAA software (version 2.0) [148]. Raw reads for 10886 genes identified by Entrez Gene ID were analyzed by GSAASeqSP, using gene set C5 (*Drosophila* version retrieved from http://www.go2msig.org/cgi-bin/prebuilt.cgi?taxid=7227) and specifying as permutation type 'gene set' and as gene set size filtering min 15 and max 800.

Western blotting and antibodies

Larval imaginal discs, pupal retinae and adult heads were dissected in cold Phosphate Buffer Saline (Na_2HPO_4 10 mM, KH_2PO_4 1.8 mM, NaCl 137 mM, KCl 2.7 mM, pH 7.4) (PBS) and then homogenized in lysis buffer (HEPES 20 mM, KCl 100 mM, Glycerol 5%, EDTA pH 8.0 10 mM, Triton-X 0.1%, DTT 1mM) freshly supplemented with Protease Inhibitors (Sigma # P8340). Protein concentration was determined with BCA analysis (Pierce # 23227). Equal amounts of proteins were loaded and separated on a 10% SDS-PAGE, then transferred on a PVDF membrane. Membranes were blocked in 10% Bovine Serum Albumin (BSA) in PBS-Tween (0.01%) for 30 minutes at 37°C. The following primary antibodies were used: rabbit anti-eIF6 (1:500, this study), rabbit anti-β-actin (1:4000, CST # 4967). To produce the anti-eIF6 antibody used in this study, a rabbit polyclonal antiserum against two epitopes on COOH-terminal peptide of eIF6 (NH2-CLSFVGMNTTATEI-COOH eIF6 203-215 aa; NH2-CATVTTKLRAALIEDMS-COOH eIF6 230-245 aa) was

prepared by Primmbiotech (Ab code: 201212-00003 GHA/12), purified in a CNBr-Sepharose column and tested for its specificity against a mix of synthetic peptides with ELISA test. The following secondary antibodies were used: donkey anti-mouse IgG HRP (1:5000, Amersham # NA931) and donkey anti-rabbit IgG HRP (1:5000, Amersham # NA934).

SUnSET Assay

Larval imaginal eye and wing discs were dissected in complete Schneider medium, and treated ex vivo with puromycin (50 µg/mL) for 30 minutes at room temperature, then fixed in 3% paraformaldehyde (PFA) for 1 hour at room temperature. Immunofluorescences were then performed as described below, using a mouse anti Puromycin (1:500 Merck Millipore # MABE343) as a primary antibody. Discs were then examined by confocal microscope (Leica SP5) and fluorescence intensity was measured with ImageJ software. For protein synthesis measurement in HEK293T cells, after 48 hours of transfection with the pcDNA3.1-eIF6 or the empty vector, we followed the adapted SUnSET protocol described in [149]. All experiments were performed at least three times, in triplicate.

Cells count

GMRGAL4/+ and GMR>DeIF6 pupal retinae at 40h APF were dissected, fixed, and stained with anti-Armadillo to count cells, as previously described (Cordero et al., 2004). Cells contained within a hexagonal array (an imaginary hexagon that connects the centres of the surrounding six ommatidia) were counted; for different genotypes, the number of cells per hexagon was calculated by counting cells, compared with corresponding control. Cells at the boundaries between neighbouring ommatidia count half. At least 3 hexagons (equivalent to 9 full ommatidia) were counted for each genotype, and phenotypes were analysed. Standard Deviation (SD) was used as statistical analysis.

Immunofluorescences, antibodies and TUNEL Assay

Larval imaginal discs and pupal retinae were dissected in cold PBS and fixed in 3% paraformaldehyde (PFA) for 1 hour at room temperature, then washed twice with

PBS and blocked in PBTB (PBS, Triton 0.3%, 5% Normal Goat Serum and 2% Bovine Serum Albumin) for 3 hours at room temperature. Primary antibodies were diluted in PBTB solution and incubated O/N at 4°C. After three washes with PBS, tissues were incubated O/N at 4°C with secondary antibodies and DAPI (1:1000, Molecular Probes # D3571) in PBS. After three washes with PBS, eye imaginal discs and retinae were mounted on slides with ProLong Gold (LifeTechnologies # P36930). The following primary antibodies were used: rabbit anti-eIF6 (1:50, this study), rat anti-ELAV (1:100, Developmental Study Hybridoma Bank DSHB # 7E8A10), mouse anti-CUT (1:100, DSHB # 2B10), mouse anti-Rough (1:100, DSHB # ro-62C2A8), mouse anti-Armadillo (1:100, DSHB # N27A), mouse anti-Chaoptin (1:100, DSHB # 24B10), rabbit anti- Dcp-1 (1:50, CST # 9578), mouse anti-Puromycin (1:500, Merck Millipore # MABE343). The following secondary antibodies were used: donkey anti-rat, donkey anti-mouse, donkey anti-rabbit (1:500 Alexa Fluor®secondary antibodies, Molecular Probes). Dead cells were detected using the In Situ Cell Death Detection Kit TMR Red (Roche # 12156792910) as manufacturer protocol, with some optimization. Briefly, retinae of the selected developmental stage were dissected in cold PBS and fixed with PFA 3% for 1 hour at room temperature. After three washes in PBS, retinae were permeabilized with Sodium Citrate 0.1%-Triton-X 0.1% for 2 minutes at 4°C, and then incubated overnight at 37°C with the enzyme mix. Retinae were then rinsed three times with PBS, incubated with DAPI to stain nuclei and mounted on slides. Discs and retinae were examined by confocal microscopy (Leica SP5) and analysed with Volocity 6.3 software (Perkin Elmer). All immunofluorescences were performed at least on three independent experiments.

Semithin sections

Semithin sections were prepared as described in [150]. Adult eyes were fixed in 0.1 M Sodium Phosphate Buffer, 2% glutaraldehyde, on ice for 30 min, then incubated with 2% OsO_4 in 0.1 M Sodium Phosphate Buffer for 2 hours on ice, dehydrated in ethanol (30%, 50%, 70%, 90%, and 100%) and twice in propylene oxide. Dehydrated eyes were then incubated O/N in 1:1 mix of propylene oxide and epoxy resin (Sigma,

Durcupan™ACM). Finally, eyes were embedded in pure epoxy resin and baked O/N at 70°C. The embedded eyes were cut on a Leica UltraCut UC6 microtome using a glass knife and images were acquired with a 100X oil lens, Nikon Upright XP61 microscope.

Ecdysone treatment

For ecdysone treatment, 20-HydroxyEcdysone (20HE) (Sigma # H5142) was dissolved in 100% ethanol to a final concentration of 5 mg/mL; third instar larvae from different genotypes (GMRGAL4/+ and GMR>DeIF6) were collected and placed in individual vials on fresh standard cornmeal food supplemented with 240 µg/mL 20-HE. Eye phenotype was analyzed in adult flies, and images were captured with a TOUPCAM™Digital camera. Eye images were analyzed with ImageJ software.

In vitro Ribosome Interaction Assay (iRIA)

iRIA assay was performed as described in [151]. Briefly, 96-well plates were coated with a cellular extract diluted in 50 µL of PBS, 0.01% Tween-20 O/N at 4 °C in humid chamber. Coating solution was removed and aspecific sites were blocked with 10% BSA, dissolved in PBS, 0.01% Tween-20 for 30 minutes at 37 °C. Plates were washed with 100 µL/well with PBS-Tween. 0.5µg of recombinant biotynilated eIF6 were resuspended in a reaction mix: 2.5 mM $MgCl_2$, 2% DMSO and PBS-0.01% Tween, to reach 50µL of final volume/well, added to the well and incubated with coated ribosomes for 1 hour at room temperature. To remove unbound proteins, each well was washed 3 times with PBS, 0.01% Tween-20. HRP-conjugated streptavidine was diluted 1:7000 in PBS, 0.01% Tween-20 and incubated in the well, 30 minutes at room temperature, in a final volume of 50 µL. Excess of streptavidine was removed through three washes with PBS-Tween. OPD (o-phenylenediamine dihydrochloride) was used according to the manufacturer's protocol (Sigma-Aldrich) as a soluble substrate for the detection of streptavidine peroxidase activity. The signal was detected after the incubation, plates were read at 450nm on a multiwell plate reader (Microplate Bio-Rad model 680). This experiment was performed at least three times, in triplicate.

HDACs activity

HDACs activity was measured with the fluorometric HDAC Activity Assay kit (Sigma # CS1010-1KT) according to the manufacturer's instructions. Briefly, cells were lysed with a buffer containing 50 mM HEPES, 150 mM NaCl, and 0.1% Triton X-100 supplemented with fresh protease inhibitors. 20 µg of cell lysates were incubated with assay buffer containing the HDACs substrate for 30 minutes at 30°C. The reaction was terminated, and the fluorescence intensity was measured in a fluorescence plate reader with Ex.=350-380nm and Em.=440-460nm.

Statistical Analysis

Each experiment was repeated at least three times, as biological replicates; means and standard deviations between different experiments were calculated. Statistical p-values obtained by Student t-test were indicated: three asterisks *** for p-values less than 0.001, two asterisks ** for p-values less than 0.01 and one asterisks * for p-values less than 0.05.

Bibliography

[1] Micheline Fromont-Racine et al. “Ribosome assembly in eukaryotes”. eng. In: *Gene* 313 (Aug. 2003), pp. 17–42.

[2] Dieter Kressler, Ed Hurt, and Jochen Bassler. “Driving ribosome assembly”. eng. In: *Biochim. Biophys. Acta* 1803.6 (June 2010), pp. 673–683.

[3] J. R. Warner. “The economics of ribosome biosynthesis in yeast”. eng. In: *Trends Biochem. Sci.* 24.11 (Nov. 1999), pp. 437–440.

[4] J. Bodem et al. “TIF-IA, the factor mediating growth-dependent control of ribosomal RNA synthesis, is the mammalian homolog of yeast Rrn3p”. eng. In: *EMBO Rep.* 1.2 (Aug. 2000), pp. 171–175.

[5] Ingrid Grummt and Craig S. Pikaard. “Epigenetic silencing of RNA polymerase I transcription”. eng. In: *Nat. Rev. Mol. Cell Biol.* 4.8 (Aug. 2003), pp. 641–649.

[6] J. Venema and D. Tollervey. “Ribosome synthesis in Saccharomyces cerevisiae”. eng. In: *Annu. Rev. Genet.* 33 (1999), pp. 261–311.

[7] Danièle Hernandez-Verdun and Pascal Roussel. “Regulators of nucleolar functions”. eng. In: *Prog Cell Cycle Res* 5 (2003), pp. 301–308.

[8] Daniel H. Lackner and Jürg Bähler. “Translational control of gene expression from transcripts to transcriptomes”. eng. In: *Int Rev Cell Mol Biol* 271 (2008), pp. 199–251.

[9] F. Buttgereit and M. D. Brand. “A hierarchy of ATP-consuming processes in mammalian cells”. eng. In: *Biochem. J.* 312 (Pt 1) (Nov. 1995), pp. 163–167.

[10] Martin Holcik and Tatyana V. Pestova. “Translation mechanism and regulation: old players, new concepts. Meeting on translational control and non-coding RNA”. eng. In: *EMBO Rep.* 8.7 (July 2007), pp. 639–643.

[11] Fátima Gebauer and Matthias W. Hentze. “Molecular mechanisms of translational control”. eng. In: *Nat. Rev. Mol. Cell Biol.* 5.10 (Oct. 2004), pp. 827–835.

[12] Deborah Silvera, Silvia C. Formenti, and Robert J. Schneider. “Translational control in cancer”. eng. In: *Nat. Rev. Cancer* 10.4 (Apr. 2010), pp. 254–266.

[13] F. Loreni, M. Mancino, and S. Biffo. “Translation factors and ribosomal proteins control tumor onset and progression: how?” eng. In: *Oncogene* 33.17 (Apr. 2014), pp. 2145–2156.

[14] Nahum Sonenberg. “eIF4E, the mRNA cap-binding protein: from basic discovery to translational research”. eng. In: *Biochem. Cell Biol.* 86.2 (Apr. 2008), pp. 178–183.

[15] Davide Ruggero. “Translational control in cancer etiology”. eng. In: *Cold Spring Harb Perspect Biol* 5.2 (Feb. 2013).

[16] S. Biffo et al. “Isolation of a novel beta4 integrin-binding protein (p27(BBP)) highly expressed in epithelial cells”. eng. In: *J. Biol. Chem.* 272.48 (Nov. 1997), pp. 30314–30321.

[17] C. M. Groft et al. “Crystal structures of ribosome anti-association factor IF6”. eng. In: *Nat. Struct. Biol.* 7.12 (Dec. 2000), pp. 1156–1164.

[18] Sebastian Klinge et al. “Crystal structure of the eukaryotic 60S ribosomal subunit in complex with initiation factor 6”. eng. In: *Science* 334.6058 (Nov. 2011), pp. 941–948.

[19] D. M. Valenzuela, A. Chaudhuri, and U. Maitra. “Eukaryotic ribosomal subunit anti-association activity of calf liver is contained in a single polypeptide chain protein of Mr = 25,500 (eukaryotic initiation factor 6)”. eng. In: *J. Biol. Chem.* 257.13 (July 1982), pp. 7712–7719.

[20] D. W. Russell and L. L. Spremulli. “Mechanism of action of the wheat germ ribosome dissociation factor: interaction with the 60 S subunit”. eng. In: *Arch. Biochem. Biophys.* 201.2 (May 1980), pp. 518–526.

[21] Chi C. Wong et al. “Defective ribosome assembly in Shwachman-Diamond syndrome”. eng. In: *Blood* 118.16 (Oct. 2011), pp. 4305–4312.

[22] Cyril Bussiere et al. “Integrity of the P-site is probed during maturation of the 60S ribosomal subunit”. eng. In: *J. Cell Biol.* 197.6 (June 2012), pp. 747–759.

[23] Marcello Ceci et al. “Release of eIF6 (p27BBP) from the 60S subunit allows 80S ribosome assembly”. eng. In: *Nature* 426.6966 (Dec. 2003), pp. 579–584.

[24] Viviana Volta et al. “RACK1 depletion in a mouse model causes lethality, pigmentation deficits and reduction in protein synthesis efficiency”. eng. In: *Cell. Mol. Life Sci.* 70.8 (Apr. 2013), pp. 1439–1450.

[25] Daniela Brina et al. “Translational control by 80S formation and 60S availability: the central role of eIF6, a rate limiting factor in cell cycle progression and tumorigenesis”. eng. In: *Cell Cycle* 10.20 (Oct. 2011), pp. 3441–3446.

[26] Andrew J. Finch et al. “Uncoupling of GTP hydrolysis from eIF6 release on the ribosome causes Shwachman-Diamond syndrome”. eng. In: *Genes Dev.* 25.9 (May 2011), pp. 917–929.

[27] Annarita Miluzio et al. “Eukaryotic initiation factor 6 mediates a continuum between 60S ribosome biogenesis and translation”. eng. In: *EMBO Rep.* 10.5 (May 2009), pp. 459–465.

[28] A. Donadini et al. “The human ITGB4BP gene is constitutively expressed in vitro, but highly modulated in vivo”. eng. In: *Gene* 266.1-2 (Mar. 2001), pp. 35–43.

[29] Dario Benelli et al. “The translation factor eIF6 is a Notch-dependent regulator of cell migration and invasion”. eng. In: *PLoS ONE* 7.2 (2012), e32047.

[30] Björn Schwanhäusser et al. “Global quantification of mammalian gene expression control”. eng. In: *Nature* 473.7347 (May 2011), pp. 337–342.

[31] Nathaniel Robichaud and Nahum Sonenberg. “Translational control and the cancer cell response to stress”. eng. In: *Curr. Opin. Cell Biol.* 45 (Apr. 2017), pp. 102–109.

[32] A. Lazaris-Karatzas, K. S. Montine, and N. Sonenberg. “Malignant transformation by a eukaryotic initiation factor subunit that binds to mRNA 5’ cap”. eng. In: *Nature* 345.6275 (June 1990), pp. 544–547.

[33] A. De Benedetti and A. L. Harris. “eIF4E expression in tumors: its possible role in progression of malignancies”. eng. In: *Int. J. Biochem. Cell Biol.* 31.1 (Jan. 1999), pp. 59–72.

[34] Janet L. Oblinger et al. “Components of the eIF4F complex are potential therapeutic targets for malignant peripheral nerve sheath tumors and vestibular schwannomas”. en. In: *Neuro-Oncology* 18.9 (Sept. 2016), pp. 1265–1277.

[35] Elena Martínez-Sáez et al. “peIF4E as an independent prognostic factor and a potential therapeutic target in diffuse infiltrating astrocytomas”. eng. In: *Cancer Med* 5.9 (Sept. 2016), pp. 2501–2512.

[36] Julia H. Carter et al. “Phosphorylation of eIF4E serine 209 is associated with tumour progression and reduced survival in malignant melanoma”. eng. In: *Br. J. Cancer* 114.4 (2016), pp. 444–453.

[37] Paola Rosso et al. “Overexpression of p27BBP in head and neck carcinomas and their lymph node metastases”. eng. In: *Head Neck* 26.5 (May 2004), pp. 408–417.

[38] Berta Martín et al. “Functional clustering of metastasis proteins describes plastic adaptation resources of breast-cancer cells to new microenvironments”. eng. In: *J. Proteome Res.* 7.8 (Aug. 2008), pp. 3242–3253.

[39] Michael N. Harris et al. “Comparative proteomic analysis of all-trans-retinoic acid treatment reveals systematic posttranscriptional control mechanisms in acute promyelocytic leukemia”. eng. In: *Blood* 104.5 (Sept. 2004), pp. 1314–1323.

[40] Annarita Miluzio et al. “Expression and activity of eIF6 trigger malignant pleural mesothelioma growth in vivo”. eng. In: *Oncotarget* 6.35 (Nov. 2015), pp. 37471–37485.

[41] Michael L. Gatza et al. “An integrated genomics approach identifies drivers of proliferation in luminal-subtype human breast cancer”. eng. In: *Nat. Genet.* 46.10 (Oct. 2014), pp. 1051–1059.

[42] Valentina Gandin et al. “Eukaryotic initiation factor 6 is rate-limiting in translation, growth and transformation”. eng. In: *Nature* 455.7213 (Oct. 2008), pp. 684–688.

[43] Annarita Miluzio et al. “Impairment of cytoplasmic eIF6 activity restricts lymphomagenesis and tumor progression without affecting normal growth”. eng. In: *Cancer Cell* 19.6 (June 2011), pp. 765–775.

[44] Daniela Brina et al. “eIF6 coordinates insulin sensitivity and lipid metabolism by coupling translation to transcription”. eng. In: *Nat Commun* 6 (Sept. 2015), p. 8261.

[45] F. Sanvito et al. “Expression of a highly conserved protein, p27BBP, during the progression of human colorectal cancer”. eng. In: *Cancer Res.* 60.3 (Feb. 2000), pp. 510–516.

[46] T. H. Morgan. “SEX LIMITED INHERITANCE IN DROSOPHILA”. eng. In: *Science* 32.812 (July 1910), pp. 120–122.

[47] C.B. Bridges and T.H. Morgan. “The third-chromosome group of mutant characters of Drosophila melanogaster.” In: *Carnegie Institute of Washington Publication* 327 (1923), pp. 1–251.

[48] C. Nüsslein-Volhard and E. Wieschaus. “Mutations affecting segment number and polarity in Drosophila”. eng. In: *Nature* 287.5785 (Oct. 1980), pp. 795–801.

[49] Berrak Ugur, Kuchuan Chen, and Hugo J. Bellen. “Drosophila tools and assays for the study of human diseases”. eng. In: *Dis Model Mech* 9.3 (Mar. 2016), pp. 235–244.

[50] M. D. Adams et al. “The genome sequence of Drosophila melanogaster”. eng. In: *Science* 287.5461 (Mar. 2000), pp. 2185–2195.

[51] Susan Tweedie et al. “FlyBase: enhancing Drosophila Gene Ontology annotations”. eng. In: *Nucleic Acids Res.* 37.Database issue (Jan. 2009), pp. D555–559.

[52] L. T. Reiter et al. “A systematic analysis of human disease-associated gene sequences in Drosophila melanogaster”. eng. In: *Genome Res.* 11.6 (June 2001), pp. 1114–1125.

[53] A. H. Brand and N. Perrimon. “Targeted gene expression as a means of altering cell fates and generating dominant phenotypes”. eng. In: *Development* 118.2 (June 1993), pp. 401–415.

[54] Daniel St Johnston. “THE ART AND DESIGN OF GENETIC SCREENS: DROSOPHILA MELANOGASTER”. In: *Nature Reviews Genetics* 3.3 (Mar. 2002), pp. 176–188.

[55] R. L. Cagan and D. F. Ready. “Notch is required for successive cell decisions in the developing Drosophila retina”. eng. In: *Genes Dev.* 3.8 (Aug. 1989), pp. 1099–1112.

[56] Jennifer Jemc and Ilaria Rebay. “Targeting Drosophila eye development”. eng. In: *Genome Biol.* 7.7 (2006), p. 226.

[57] R. C. Hardie. “Functional Organization of the Fly Retina”. In: *Progress in Sensory Physiology*. Ed. by Hansjochem Autrum et al. Vol. 5. DOI: 10.1007/978-3-642-70408-6_1. Berlin, Heidelberg: Springer Berlin Heidelberg, 1985, pp. 1–79.

[58] Thomas R. Clandinin and S. Lawrence Zipursky. “Making connections in the fly visual system”. eng. In: *Neuron* 35.5 (Aug. 2002), pp. 827–841.

[59] Shayan Izaddoost et al. “Drosophila Crumbs is a positional cue in photoreceptor adherens junctions and rhabdomeres”. eng. In: *Nature* 416.6877 (Mar. 2002), pp. 178–183.

[60] J. P. Kumar and D. F. Ready. “Rhodopsin plays an essential structural role in Drosophila photoreceptor development”. eng. In: *Development* 121.12 (Dec. 1995), pp. 4359–4370.

[61] C. S. Zuker, A. F. Cowman, and G. M. Rubin. “Isolation and structure of a rhodopsin gene from D. melanogaster”. eng. In: *Cell* 40.4 (Apr. 1985), pp. 851–858.

[62] W. H. Chou et al. “Patterning of the R7 and R8 photoreceptor cells of Drosophila: evidence for induced and default cell-fate specification”. eng. In: *Development* 126.4 (Feb. 1999), pp. 607–616.

[63] J. L. Haynie and P. J. Bryant. “Development of the eye-antenna imaginal disc and morphogenesis of the adult head in Drosophila melanogaster”. eng. In: *J. Exp. Zool.* 237.3 (Mar. 1986), pp. 293–308.

[64] Ross Cagan. “Principles of Drosophila eye differentiation”. eng. In: *Curr. Top. Dev. Biol.* 89 (2009), pp. 115–135.

[65] Jih-Guang Yao et al. “Differential requirements for the Pax6(5a) genes eyegone and twin of eyegone during eye development in Drosophila”. eng. In: *Dev. Biol.* 315.2 (Mar. 2008), pp. 535–551.

[66] U. Heberlein and K. Moses. “Mechanisms of Drosophila retinal morphogenesis: the virtues of being progressive”. eng. In: *Cell* 81.7 (June 1995), pp. 987–990.

[67] Justin P. Kumar. “The fly eye: Through the looking glass”. eng. In: *Dev. Dyn.* (Aug. 2017).

[68] A. Benlali et al. “act up controls actin polymerization to alter cell shape and restrict Hedgehog signaling in the Drosophila eye disc”. eng. In: *Cell* 101.3 (Apr. 2000), pp. 271–281.

[69] A. P. Jarman et al. “Atonal is the proneural gene for Drosophila photoreceptors”. eng. In: *Nature* 369.6479 (June 1994), pp. 398–400.

[70] A. P. Jarman et al. “Role of the proneural gene, atonal, in formation of Drosophila chordotonal organs and photoreceptors”. eng. In: *Development* 121.7 (July 1995), pp. 2019–2030.

[71] J. C. de Nooij and I. K. Hariharan. “Uncoupling cell fate determination from patterned cell division in the Drosophila eye”. eng. In: *Science* 270.5238 (Nov. 1995), pp. 983–985.

[72] Justin P. Kumar. “My what big eyes you have: how the Drosophila retina grows”. eng. In: *Dev Neurobiol* 71.12 (Dec. 2011), pp. 1133–1152.

[73] T. Wolff and D. F. Ready. “The beginning of pattern formation in the Drosophila compound eye: the morphogenetic furrow and the second mitotic wave”. eng. In: *Development* 113.3 (Nov. 1991), pp. 841–850.

[74] W. Fu and M. Noll. “The Pax2 homolog sparkling is required for development of cone and pigment cells in the Drosophila eye”. eng. In: *Genes Dev.* 11.16 (Aug. 1997), pp. 2066–2078.

[75] W. Fu et al. “shaven and sparkling are mutations in separate enhancers of the Drosophila Pax2 homolog”. eng. In: *Development* 125.15 (Aug. 1998), pp. 2943–2950.

[76] Yandong Shi and Markus Noll. “Determination of cell fates in the R7 equivalence group of the Drosophila eye by the concerted regulation of D-Pax2 and TTK88”. eng. In: *Dev. Biol.* 331.1 (July 2009), pp. 68–77.

[77] R. L. Cagan and D. F. Ready. “The emergence of order in the Drosophila pupal retina”. eng. In: *Dev. Biol.* 136.2 (Dec. 1989), pp. 346–362.

[78] Raghavendra Nagaraj and Utpal Banerjee. “Combinatorial signaling in the specification of primary pigment cells in the Drosophila eye”. eng. In: *Development* 134.5 (Mar. 2007), pp. 825–831.

[79] Serena J. Silver and Ilaria Rebay. “Signaling circuitries in development: insights from the retinal determination gene network”. eng. In: *Development* 132.1 (Jan. 2005), pp. 3–13.

[80] S. B. Tanenbaum et al. “A screen for dominant modifiers of the irreC-rst cell death phenotype in the developing Drosophila retina”. eng. In: *Genetics* 156.1 (Sept. 2000), pp. 205–217.

[81] Nicolas Dos-Santos et al. “Drosophila retinal pigment cell death is regulated in a position-dependent manner by a cell memory gene”. eng. In: *Int. J. Dev. Biol.* 52.1 (2008), pp. 21–31.

[82] Carrie Baker Brachmann and Ross L. Cagan. “Patterning the fly eye: the role of apoptosis”. eng. In: *Trends Genet.* 19.2 (Feb. 2003), pp. 91–96.

[83] D. L. Vaux and S. J. Korsmeyer. “Cell death in development”. eng. In: *Cell* 96.2 (Jan. 1999), pp. 245–254.

[84] Ingrid Böhm and Hans Schild. “Apoptosis: the complex scenario for a silent cell death”. eng. In: *Mol Imaging Biol* 5.1 (Feb. 2003), pp. 2–14.

[85] N. Inohara et al. “CLARP, a death effector domain-containing protein interacts with caspase-8 and regulates apoptosis”. eng. In: *Proc. Natl. Acad. Sci. U.S.A.* 94.20 (Sept. 1997), pp. 10717–10722.

[86] P. Chen et al. “Dredd, a novel effector of the apoptosis activators reaper, grim, and hid in Drosophila”. eng. In: *Dev. Biol.* 201.2 (Sept. 1998), pp. 202–216.

[87] L. Dorstyn et al. “DRONC, an ecdysone-inducible Drosophila caspase”. eng. In: *Proc. Natl. Acad. Sci. U.S.A.* 96.8 (Apr. 1999), pp. 4307–4312.

[88] Sun-Yun Yu et al. “A pathway of signals regulating effector and initiator caspases in the developing Drosophila eye”. eng. In: *Development* 129.13 (July 2002), pp. 3269–3278.

[89] Loretta Dorstyn et al. “The role of cytochrome c in caspase activation in Drosophila melanogaster cells”. eng. In: *J. Cell Biol.* 156.6 (Mar. 2002), pp. 1089–1098.

[90] C. J. Hawkins et al. “The Drosophila caspase DRONC cleaves following glutamate or aspartate and is regulated by DIAP1, HID, and GRIM”. eng. In: *J. Biol. Chem.* 275.35 (Sept. 2000), pp. 27084–27093.

[91] B. A. Hay. “Understanding IAP function and regulation: a view from Drosophila”. eng. In: *Cell Death Differ.* 7.11 (Nov. 2000), pp. 1045–1056.

[92] Sally Kornbluth and Kristin White. “Apoptosis in Drosophila: neither fish nor fowl (nor man, nor worm)”. eng. In: *J. Cell. Sci.* 118.Pt 9 (May 2005), pp. 1779–1787.

[93] C. Jiang et al. “A steroid-triggered transcriptional hierarchy controls salivary gland cell death during Drosophila metamorphosis”. eng. In: *Mol. Cell* 5.3 (Mar. 2000), pp. 445–455.

[94] Yanping Zhang et al. “Epigenetic blocking of an enhancer region controls irradiation-induced proapoptotic gene expression in Drosophila embryos”. eng. In: *Dev. Cell* 14.4 (Apr. 2008), pp. 481–493.

[95] Ingrid Lohmann et al. “The Drosophila Hox gene deformed sculpts head morphology via direct regulation of the apoptosis activator reaper”. eng. In: *Cell* 110.4 (Aug. 2002), pp. 457–466.

[96] S. L. Wang et al. “The Drosophila caspase inhibitor DIAP1 is essential for cell survival and is negatively regulated by HID”. eng. In: *Cell* 98.4 (Aug. 1999), pp. 453–463.

[97] Soon Ji Yoo et al. “Hid, Rpr and Grim negatively regulate DIAP1 levels through distinct mechanisms”. eng. In: *Nat. Cell Biol.* 4.6 (June 2002), pp. 416–424.

[98] Rebecca Hays, Laura Wickline, and Ross Cagan. “Morgue mediates apoptosis in the Drosophila melanogaster retina by promoting degradation of DIAP1”. eng. In: *Nat. Cell Biol.* 4.6 (June 2002), pp. 425–431.

[99] C. Reiter et al. “Reorganization of membrane contacts prior to apoptosis in the Drosophila retina: the role of the IrreC-rst protein”. eng. In: *Development* 122.6 (June 1996), pp. 1931–1940.

[100] Sujin Bao and Ross Cagan. “Preferential adhesion mediated by Hibris and Roughest regulates morphogenesis and patterning in the Drosophila eye”. eng. In: *Dev. Cell* 8.6 (June 2005), pp. 925–935.

[101] R. G. Ramos et al. “The irregular chiasm C-roughest locus of Drosophila, which affects axonal projections and programmed cell death, encodes a novel immunoglobulin-like protein”. eng. In: *Genes Dev.* 7.12B (Dec. 1993), pp. 2533–2547.

[102] J. W. Barclay and R. M. Robertson. “Role for calcium in heat shock-mediated synaptic thermoprotection in Drosophila larvae”. eng. In: *J. Neurobiol.* 56.4 (Sept. 2003), pp. 360–371.

[103] R. O. Hynes and A. D. Lander. “Contact and adhesive specificities in the associations, migrations, and targeting of cells and axons”. eng. In: *Cell* 68.2 (Jan. 1992), pp. 303–322.

[104] Gina-Marie Barletta et al. “Nephrin and Neph1 co-localize at the podocyte foot process intercellular junction and form cis hetero-oligomers”. eng. In: *J. Biol. Chem.* 278.21 (May 2003), pp. 19266–19271.

[105] J. C. Rusconi, R. Hays, and R. L. Cagan. “Programmed cell death and patterning in Drosophila”. eng. In: *Cell Death Differ.* 7.11 (Nov. 2000), pp. 1063–1070.

[106] D. T. Miller and R. L. Cagan. “Local induction of patterning and programmed cell death in the developing Drosophila retina”. eng. In: *Development* 125.12 (June 1998), pp. 2327–2335.

[107] N. E. Baker and S. Y. Yu. “The EGF receptor defines domains of cell cycle progression and survival to regulate cell number in the developing Drosophila eye”. eng. In: *Cell* 104.5 (Mar. 2001), pp. 699–708.

[108] K. Sawamoto et al. “Argos induces programmed cell death in the developing Drosophila eye by inhibition of the Ras pathway”. eng. In: *Cell Death Differ.* 5.4 (Apr. 1998), pp. 262–270.

[109] Jill Wildonger et al. “Lozenge directly activates argos and klumpfuss to regulate programmed cell death”. eng. In: *Genes Dev.* 19.9 (May 2005), pp. 1034–1039.

[110] M. Freeman. “Misexpression of the Drosophila argos gene, a secreted regulator of cell determination”. eng. In: *Development* 120.8 (Aug. 1994), pp. 2297–2304.

[111] S. M. Gorski et al. “Delta and notch promote correct localization of irreC-rst”. eng. In: *Cell Death Differ.* 7.10 (Oct. 2000), pp. 1011–1013.

[112] R. J. Denver et al. “Comparative endocrinology in the 21st century”. en. In: *Integrative and Comparative Biology* 49.4 (Oct. 2009), pp. 339–348.

[113] L. M. Riddiford. “Hormone receptors and the regulation of insect metamorphosis”. eng. In: *Receptor* 3.3 (1993), pp. 203–209.

[114] G. Richards. “The radioimmune assay of ecdysteroid titres in Drosophila melanogaster”. eng. In: *Mol. Cell. Endocrinol.* 21.3 (Mar. 1981), pp. 181–197.

[115] M. Ashburner. “Sequential gene activation by ecdysone in polytene chromosomes of Drosophila melanogaster. II. The effects of inhibitors of protein synthesis”. eng. In: *Dev. Biol.* 39.1 (July 1974), pp. 141–157.

[116] Lawrence I. Gilbert, Robert Rybczynski, and James T. Warren. “Control and biochemical nature of the ecdysteroidogenic pathway”. eng. In: *Annu. Rev. Entomol.* 47 (2002), pp. 883–916.

[117] Lawrence I. Gilbert. “Halloween genes encode P450 enzymes that mediate steroid hormone biosynthesis in Drosophila melanogaster”. eng. In: *Mol. Cell. Endocrinol.* 215.1-2 (Feb. 2004), pp. 1–10.

[118] Yanhui Xiang, Zhonghua Liu, and Xun Huang. “br regulates the expression of the ecdysone biosynthesis gene npc1”. eng. In: *Dev. Biol.* 344.2 (Aug. 2010), pp. 800–808.

[119] Stephen L. Sturley et al. “The pathophysiology and mechanisms of NP-C disease”. eng. In: *Biochim. Biophys. Acta* 1685.1-3 (Oct. 2004), pp. 83–87.

[120] Takuji Yoshiyama-Yanagawa et al. “The conserved Rieske oxygenase DAF-36/Neverland is a novel cholesterol-metabolizing enzyme”. eng. In: *J. Biol. Chem.* 286.29 (July 2011), pp. 25756–25762.

[121] Ryusuke Niwa et al. “Non-molting glossy/shroud encodes a short-chain dehydrogenase/reductase that functions in the ’Black Box’ of the ecdysteroid biosynthesis pathway”. eng. In: *Development* 137.12 (June 2010), pp. 1991–1999.

[122] Anna Petryk et al. “Shade is the Drosophila P450 enzyme that mediates the hydroxylation of ecdysone to the steroid insect molting hormone 20-hydroxyecdysone”. eng. In: *Proc. Natl. Acad. Sci. U.S.A.* 100.24 (Nov. 2003), pp. 13773–13778.

[123] H. E. Thomas, H. G. Stunnenberg, and A. F. Stewart. “Heterodimerization of the Drosophila ecdysone receptor with retinoid X receptor and ultraspiracle”. eng. In: *Nature* 362.6419 (Apr. 1993), pp. 471–475.

[124] V. C. Henrich et al. “A steroid/thyroid hormone receptor superfamily member in Drosophila melanogaster that shares extensive sequence similarity with a mammalian homologue”. eng. In: *Nucleic Acids Res.* 18.14 (July 1990), pp. 4143–4148.

[125] W. S. Talbot, E. A. Swyryd, and D. S. Hogness. “Drosophila tissues with different metamorphic responses to ecdysone express different ecdysone receptor isoforms”. eng. In: *Cell* 73.7 (July 1993), pp. 1323–1337.

[126] M. Ashburner. “Puffs, genes, and hormones revisited”. eng. In: *Cell* 61.1 (Apr. 1990), pp. 1–3.

[127] C. S. Thummel, K. C. Burtis, and D. S. Hogness. “Spatial and temporal patterns of E74 transcription during Drosophila development”. eng. In: *Cell* 61.1 (Apr. 1990), pp. 101–111.

[128] W. A. Segraves and D. S. Hogness. “The E75 ecdysone-inducible gene responsible for the 75B early puff in Drosophila encodes two new members of the steroid receptor superfamily”. eng. In: *Genes Dev.* 4.2 (Feb. 1990), pp. 204–219.

[129] Yunsik Kang and Arash Bashirullah. “A steroid-controlled global switch in sensitivity to apoptosis during Drosophila development”. eng. In: *Dev. Biol.* 386.1 (Feb. 2014), pp. 34–41.

[130] T. J. Daish, D. Cakouros, and S. Kumar. “Distinct promoter regions regulate spatial and temporal expression of the Drosophila caspase dronc”. eng. In: *Cell Death Differ.* 10.12 (Dec. 2003), pp. 1348–1356.

[131] Alberto del Valle Rodríguez, Dominic Didiano, and Claude Desplan. “Power tools for gene expression and clonal analysis in Drosophila”. eng. In: *Nat. Methods* 9.1 (Dec. 2011), pp. 47–55.

[132] Justin P. Kumar. “Building an ommatidium one cell at a time”. eng. In: *Dev. Dyn.* 241.1 (Jan. 2012), pp. 136–149.

[133] Niraj Shenoy et al. “Alterations in the ribosomal machinery in cancer and hematologic disorders”. eng. In: *J Hematol Oncol* 5 (June 2012), p. 32.

[134] Mamatha Bhat et al. “Targeting the translation machinery in cancer”. eng. In: *Nat Rev Drug Discov* 14.4 (Apr. 2015), pp. 261–278.

[135] Jennifer Chu et al. “Translation Initiation Factors: Reprogramming Protein Synthesis in Cancer”. eng. In: *Trends Cell Biol.* 26.12 (Dec. 2016), pp. 918–933.

[136] Kaveh M. Goudarzi and Mikael S. Lindström. “Role of ribosomal protein mutations in tumor development (Review)”. eng. In: *Int. J. Oncol.* 48.4 (Apr. 2016), pp. 1313–1324.

[137] Daniela Brina et al. “eIF6 anti-association activity is required for ribosome biogenesis, translational control and tumor progression”. eng. In: *Biochim. Biophys. Acta* 1849.7 (July 2015), pp. 830–835.

[138] S. Ricciardi et al. “Eukaryotic translation initiation factor 6 is a novel regulator of reactive oxygen species-dependent megakaryocyte maturation”. eng. In: *J. Thromb. Haemost.* 13.11 (Nov. 2015), pp. 2108–2118.

[139] N. De Marco et al. “p27(BBP)/eIF6 acts as an anti-apoptotic factor upstream of Bcl-2 during Xenopus laevis development”. eng. In: *Cell Death Differ.* 17.2 (Feb. 2010), pp. 360–372.

[140] Barbara N. Borsos et al. “Acetylations of Ftz-F1 and histone H4K5 are required for the fine-tuning of ecdysone biosynthesis during Drosophila metamorphosis”. eng. In: *Dev. Biol.* 404.1 (Aug. 2015), pp. 80–87.

[141] T. Pankotai et al. “Genes of the ecdysone biosynthesis pathway are regulated by the dATAC histone acetyltransferase complex in Drosophila”. eng. In: *Mol. Cell. Biol.* 30.17 (Sept. 2010), pp. 4254–4266.

[142] Lucia Daxinger et al. “A forward genetic screen identifies eukaryotic translation initiation factor 3, subunit H (eIF3h), as an enhancer of variegation in the mouse”. eng. In: *G3 (Bethesda)* 2.11 (Nov. 2012), pp. 1393–1396.

[143] Y. Ji et al. “Eukaryotic initiation factor 6 selectively regulates Wnt signaling and beta-catenin protein synthesis”. eng. In: *Oncogene* 27.6 (Jan. 2008), pp. 755–762.

[144] Anthony M. Bolger, Marc Lohse, and Bjoern Usadel. “Trimmomatic: a flexible trimmer for Illumina sequence data”. eng. In: *Bioinformatics* 30.15 (Aug. 2014), pp. 2114–2120.

[145] Alexander Dobin et al. “STAR: ultrafast universal RNA-seq aligner”. eng. In: *Bioinformatics* 29.1 (Jan. 2013), pp. 15–21.

[146] Simon Anders, Paul Theodor Pyl, and Wolfgang Huber. “HTSeq–a Python framework to work with high-throughput sequencing data”. eng. In: *Bioinformatics* 31.2 (Jan. 2015), pp. 166–169.

[147] Michael I. Love, Wolfgang Huber, and Simon Anders. “Moderated estimation of fold change and dispersion for RNA-seq data with DESeq2”. eng. In: *Genome Biol.* 15.12 (2014), p. 550.

[148] Qing Xiong, Sayan Mukherjee, and Terrence S. Furey. “GSAASeqSP: a toolset for gene set association analysis of RNA-Seq data”. eng. In: *Sci Rep* 4 (Sept. 2014), p. 6347.

[149] Piera Calamita et al. “SBDS-Deficient Cells Have an Altered Homeostatic Equilibrium due to Translational Inefficiency Which Explains their Reduced Fitness and Provides a Logical Framework for Intervention”. en. In: *PLOS Genetics* 13.1 (Jan. 2017). Ed. by Gregory P. Copenhaver, e1006552.

[150] Silvia Montrasio, Marek Mlodzik, and Manolis Fanto. “A new allele uncovers the role of echinus in the control of ommatidial rotation in the Drosophila eye”. eng. In: *Dev. Dyn.* 236.10 (Oct. 2007), pp. 2936–2942.

[151] Elisa Pesce et al. “Direct and high throughput (HT) interactions on the ribosomal surface by iRIA”. eng. In: *Sci Rep* 5 (Oct. 2015), p. 15401.

Ringraziamenti

Gli ultimi tre anni sono stati un'esperienza impegnativa, intorno a cui la mia vita ha completamente ruotato, coinvolgendo ogni aspetto della mia quotidianità. Ha richiesto la mia più completa dedizione, ogni briciolo di energia. In cambio, però, sono convinta di aver ricevuto altrettanto, forse anche qualcosa in più. Il dottorato di ricerca mi ha insegnato un mestiere, senza dubbio il più bello del mondo. Ma soprattutto, il dottorato di ricerca mi ha fatto diventare adulta, smussando alcuni difetti, facendone emergere altri, insegnandomi a correggerli ogni giorno. Tutto questo non sarebbe stato possibile senza l'aiuto di tante persone, così tante che queste poche righe inevitabilmente non saranno in grado di contenere.

Prima di tutto grazie alla mia famiglia: non avete smesso un minuto di credere in me, anche quando ero io stessa ad avere dei dubbi. Non ce l'avrei fatta senza il vostro costante supporto. Spero che questo traguardo vi ripaghi almeno in parte, anche se so che non sarà mai abbastanza.

Un grazie al Prof. Patrone, mio tutor interno, che mi ha sempre appoggiata da lontano durante questo lungo percorso.

Grazie al Prof. Biffo, che mi ha ospitato nel suo laboratorio e che non mi ha mai fatto mancare un consiglio, una parola esperta. Potrà sembrargli che non sempre abbia recepito i suoi suggerimenti, non solo lavorativi, ma spero sappia che ne ho sempre fatto tesoro.

Devo ringraziare tutti i ragazzi del laboratorio MHCG della Fondazione INGM: tre anni in un ambiente giovane e dinamico mi hanno permesso di intrecciare anche amicizie che spero rimarranno a lungo, anche dopo che questa esperienza sarà conclusa. Per cui grazie a Piera Calamita, Guido Gatti, Marilena Mancino, Roberta Alfieri, Alessandra Scagliola, Simone Gallo, Stefania Oliveto, Nicola Manfrini, Elisa Pesce, Sara Ricciardi, Annarita Miluzio e Sipontina Faienza.

Un grazie particolare a Guido: non avrei potuto immaginare uno studente migliore di te. Continua su questa strada e un giorno potrò dire di avere qualche merito per il tuo successo. Ad Alessandra: condividere con te una parte di questo percorso lo ha reso più lieve, più facile, più divertente. Magari la prossima volta facciamo una vacanza invece che un congresso! A Marilena: per aver condiviso idee e valori.

Non cambiare, non perdere la tua passione, è quello che ti definisce e che fa di te la persona meravigliosa che sei. A Roberta, la ragazza (magica) dei computer, grazie per aver condiviso momenti, passioni e risate.
Infine, il grazie più grande di tutti a Piera: non avrei mai immaginato di trovare una sorella in un laboratorio distante 600km da casa. Non mi hai solo guidato in questo progetto, insegnandomi tutto quello che mi serviva sapere in flyroom. Mi hai offerto una famiglia su cui appoggiarmi quando ne avevo bisogno, un porto sicuro in cui rifugiarmi. Senza di te questo percorso sarebbe stato più cupo e la via per il traguardo costellata da meno risate.
Infine, coloro che mi hanno supportato fuori dal lab: grazie a chi mi ha accolto a Milano, Vanessa, Oscar, Francesco e Roberto. Grazie a chi c'è sempre stato da lontano: Flavia, Chiara e Mariateresa.